https://doi.org/10.1016/j.tranpol.2021.11.023

Promoting Green Transportation Under the Belt and Road Initiative: Locating Charging Stations Considering Electric Vehicle Users' Travel Behaviour

*Xu Ouyang, Min Xu**

Department of Industrial and Systems Engineering, The Hong Kong Polytechnic University, Hung Hom, Hong Kong

Abstract

Motivated by the worldwide promotion of green transportation, this study aims to determine the optimal location of multi-type electric vehicle (EV) charging stations, e.g., fast and slow charging stations, for maximizing the covered traffic flows under a limited budget while considering EV users' partial charging behavior and elastic demand. A two-phase approach is proposed to efficiently solve this problem. The efficacy of the proposed two-phase approach is demonstrated by numerical experiments on the highway network of Zhejiang Province, China, and policies towards promoting transport electrification are discussed from various aspects. In particular, our policy suggestions are fivefold: (a) how to save investment in station construction by understanding EV users' tolerance for travel cost deviation; (b) how to determine the budget policy to ensure an efficient utilization of the investment; (c) how to optimally select the location and type of charging stations; (d) how to devise the operation regulations based on the workload of each station; as well as (e) how to plan the station construction in a mid- or long- term implementation. We also discuss some prospective challenges and opportunities regarding charging station construction and operations in the context of continuous innovation in energy and communication technologies such as the Internet of Things (IoT).

Keywords: green transportation, charging station location, charging behavior, policy making.

* Corresponding author
Tel: +852 2766 6593
Fax: +852 2362 5267
E-mail: xumincee@gmail.com; min.m.xu@polyu.edu.hk (M. Xu)

1. Introduction

As a green transport mode, electric vehicles (EVs) have become increasingly popular over the past decade thanks to their high energy efficiency and zero tail-pipe emissions. Due to their limited driving ranges, EV users often need to refuel energy during trips, especially on a long trip such as an inter-city journey. However, the lack of charging resources could prevent travelers from completing their travels as the battery is possibly depleted en-route. As a matter of fact, the deployment of charging facilities has been recognized as a crucial factor for the wide adoption of EVs (Franke and Krems, 2013; Lebeau et al., 2013; She et al., 2017; Sun et al., 2018). To promote the use of EVs, many governments over the world have substantially invested in building charging infrastructures (IEA, 2017). For example, respecting the environmentally friendly initiative, the Chinese government has allocated billions dedicated to constructing EV plants and charging facilities billions domestically and overseas to promote green transportation under the Belt-and-Road Initiative (BRI) (Araya, 2018). One of the prominent decision-making problems for the governments when building charging infrastructures is to determine their locations. Without careful planning, early deployment of charging stations often results in a poor fulfillment of charging demands and a low rate of facility utilization. To achieve a good demand fulfilling level under a limited budget, optimization model and algorithm design are imperative to obtain an intelligent deployment plan of charging stations.

The public charging facilities can be classified into two main types according to their charging efficiency, i.e., fast and slow charging stations (Morrow et al., 2008). A fast charging station is often equipped with DC chargers with a power larger than 50 kWh, while a slow charging station usually adopts AC chargers with a power smaller than 20 kWh (Yilmaz and Krein, 2012). Fast charging stations deliver a more efficient charging service to the EV users while it generally requires a high cost of procurement, installation, and operation; in contrast, slow charging stations are much more economical whereas their low charging efficiency could be less attractive to the travelers (Globisch et al., 2019; Liao et al., 2019; Wee et al., 2020). However, even ignoring the charging efficiency drawback, building a slow charging station still needs a huge investment. As reported by NREL (2012), the construction cost of a fast and a slow charging station is around \$8.5 million and \$4.25 million, respectively. The huge construction costs and the distinct charging efficiency of these two kinds of stations motivate the investigation of the multi-type charging station location problem.

1.1. Literature review

Extensive efforts have been made to determine the optimal location of EV charging stations and other alternative fuel vehicle refueling stations. Examples include Hodgson (1990), Kim and Kuby (2012), Kuby and Lim (2005), Owen and Daskin (1998), Revelle (1993), and Upchurch et al. (2009). Among the existing studies, Hodgson (1990) formulated users' travel demand as a path flow between an origin and destination (OD) pair for the first time. A flow was assumed to be covered if at least one refueling facility stationed along its travel path. A flow capture location model (FCLM) was developed to allocate a given number of facilities for flow coverage maximization. The FCLM was then extended by Kuby and Lim (2005) through relaxing the assumption that one refueling station along the travel path was sufficient for the entire trip. They proposed a flow refueling location model (FRLM) where the travelers may need to refuel energy many times to sustain their journeys. The travelers in both the FCLM and the FRLM were assumed to travel on the shortest path, whereas they could make a detour for energy refueling in reality (Caulfield et al., 2010). The detour behavior was then considered by Kim and Kuby (2012) in a deviation flow refueling location model (DFRLM). They assumed that any deviation path with the travel distance within a pre-specified threshold was feasible for the travelers. Since then, many other practical features were considered in charging station location and charging system designing problems, such as limited station capacity (Hosseini et al., 2017; Upchurch et al., 2009), driving range anxiety (Guo et al., 2018; Xu et al., 2020), stochastic travel demand (Hosseini and MirHassani, 2015), user equilibrium (He et al., 2018, 2020; Zheng et al., 2017), automated vehicles (Zhang et al., 2021), mobile charging (Zhang et al., 2020b), daily charging (Zhang et al., 2020a), and hybrid energy charging (Abbasi et al., 2019; Wang et al., 2019), etc. Notably, Liu and Wang (2017) investigated a cutting-edge charging mode, i.e., wireless dynamic charging. They aimed to simultaneously locate wireless dynamic charging facilities and conventional charging stations for a hierarchical objective of three levels.

The majority of these studies assumed that an EV user would fully charge the battery at the visited station regardless of the remaining state-of-charge (SOC) before charging. Fully charging a battery could be time-consuming at a slow charging station and expensive at a fast charging station. In the real world, travelers often partially charge their vehicles for the sake of cost or time savings (Schiffer and Walther, 2017; Xu et al., 2017). However, the users' partial charging behavior is rarely considered in the context of charging station location problems. In fact, formulating fully charging is already nontrivial – generally needs subtle modeling techniques and a large number of constraints. It can be imagined that incorporating partial charging in the location model can be much more demanding. Hence, how to model the partial charging behavior effectively and efficiently deserves further investigation.

Another critical observation is that, due to the limited charging resources, the EV users could suffer additional travel costs resulting from the detour behavior for battery charging. It has been found that the traffic flow would decline if the travel cost increased (Souche, 2010), which is often referred to as elastic demand in the literature (Chu et al., 2019; Commins and Nolan, 2011; Gao et al., 2021; Lu et al., 2015; Masoumi, 2019; Soltani-Sobh et al., 2017). Regarding battery charging, it is closely related to EV's energy consumption and users' charging behavior, which are largely affected by EV's own properties (Liao et al., 2021). In particular, Liao et al. (2021) used longitudinal dynamics model to study how the battery thermal impacts the battery charging and discharging, and then derive several energy-efficient EV driving strategies based on the model. The results were further tested and verified by extensive simulation. Though cost and charging behavior are critical, only Kim and Kuby (2012) and Xu and Meng (2020) have ever investigated the impact of the travel cost on EV users' travel demands in facility location problems and a logit-based form function was proposed to depict the demand elasticity. However, both of them assumed for simplicity that the EVs will be fully charged at the visited stations. A location model of multi-type charging stations considering users' partial charging behavior and the elastic demand is expected. To address this problem, Ouyang et al. (2020) recently developed a mixed-integer nonlinear programming model and obtained the ε-optimal solution by piece-wise linear approximation method. The resultant mixed-integer linear programming model was solved by MIP solvers. However, their model required a long time to be solved even for a mid-sized network. A computationally efficient approach that is applicable to large-scale problems is thus anticipated.

1.2 Objective and contributions

In this study, we aim to optimally locate multiple types of charging stations (DMCS) under a limited budget considering various practical characteristics of EV users' behavior. In particular, users can partially recharge EVs at any visited stations, and additionally, if users have to detour for recharging, the increased travel costs will nonlinearly decrease the number of users willing to choose EVs for traveling, namely, nonlinear elastic travel demand. The DMCS problem can be formulated by a mixed-integer nonlinear program. However, solving such a model, especially for real-world large-scale instances, is computationally challenging. We thus propose an efficient two-phase approach to the DMCS problem. Specifically, the first phase employs a tailored two-layer simulated annealing (TSA) algorithm to quickly find good-quality station deployment, while the second phase adopts the best deployment found in the first phase as the initial solution to the DMCS model to accelerate the procedure to find the optimal solution. It is worth noting that in the course of TSA, constructing and improving station deployment can be very time-consuming because of the nonlinear demand elasticity. Fortunately, after examining the property of the elastic demand function, we can use a simple linear mixed-integer linear model to obtain the demand quickly given a station deployment quickly. This problem-specific auxiliary model significantly saves the runtime of TSA and thus the entire two-phase approach.

The contributions of this study can be summarized by the following four perspectives:

a) *Practical problem features:* Compared with existing charging station location studies that also consider user behavior features, we investigate two practical features: partial recharging behavior and nonlinear elastic demand. To the best of our knowledge, this research pioneers in modeling the above two behaviors simultaneously in the context of EV charging station location problems.

b) *Tailored solution approach:* Modeling partial recharging and nonlinear elastic demand create difficulty in finding the optimal station deployment. By examining problem-specific properties, we propose an auxiliary mixed-integer linear model together with a two-phase solution approach. It can quickly find good station deployment and also helps accelerate the procedure to find the optimal deployment.

c) *Real-world case validation:* We use the real-world highway network, i.e., Zhejiang Province, China, to conduct substantial numerical experiments. The results show that our two-phase approach largely outperforms the state-of-the-art solver CPLEX.

d) *Important managerial implications:* The ultimate goal of this study is to provide meaningful insights to real-world operators and help them wisely locate and operate charging stations by the proposed model. To this end, we propose a five-fold policy analysis, respectively with respect to advertising green transport modes, seeking rational construction investment, prioritizing large cities in investment, differentiating operations policy for each station, and using Internet-of-Things (IoT) and Big Data technologies to enhance operations.

The remainder of this paper is organized as follows. Section 2 illustrates the assumptions and notations of the DMCS problem. Section 3 describes the two-phase approach in detail. Section 4 conducts a case study of a real-world highway network. Section 5 concludes the paper and discusses future research directions.

2. Assumptions, notations, and problem statement

Consider an EV charging service provider who has a budget B to deploy public charging stations on a highway network $G=(N, A)$, where N and A are the location set and link set, respectively. Fast and slow charging stations can be located at some pre-specified candidate locations on the network, denoted by set $S \subseteq N$. The cost of deploying a type q charging station at location $s \in S$ is denoted by b_s^q. For simplicity, we assume that the charging stations are incapacitated, and a candidate location can accommodate either a fast or a slow charging station. The EVs are assumed to be homogeneous in terms of the battery capacity E, measured in kWh. All OD pairs are grouped into a set W, which is assumed to be known in advance. The origin and destination of a particular OD pair $w \in W$ are denoted by $o(w)$ and $d(w) \in N$, respectively. The EVs will depart from location $o(w)$ with the SOC E_O at least and arrive at location $d(w)$ with the SOC above a given threshold E_D. The electricity consumption and the travel time of link $(i, j) \in A, i, j \in N$ are represented by e_{ij} and t_{ij} respectively. In the next three subsections, we will illustrate EV users' partial charging behavior, the generalized travel cost, and the elastic demand in detail. The notations used throughout this paper are summarized in Appendix 1 for readability.

2.1 Partial charging behavior

In contrast to the existing studies assuming that EVs are fully refueled at charging stations regardless of the remaining SOC, we assume the EVs can be partially replenished in each charging activity. Considering the partial charging behavior more aligns with the context of locating multi-type charging stations because the charging efficiency and prices could affect users' charging amount. By allowing partial charging, the users could refuel the energy as much as needed rather than extensively. Besides, the charging amount and cost in the fully charging behavior are generally assumed to be a pre-specified constant (Kuby and Lim, 2005). On the contrary, the charging amount is a decision variable in this study and both the charging cost and charging time will be linearly proportional to the charging amount. To formulate the charging amount and the change of SOC, for each OD pair $w \in W$, we define a binary variable $r_s^w, \forall s \in S$ denoting whether the travelers of OD pair w charge at location s, a continuous variable $p_s^w, \forall s \in S$ representing the charging amount at location s, and a continuous variable e_i^w expressing the SOC upon leaving location $i, \forall i \in N$.

2.2 Generalized travel costs

The cost of a trip mainly consists of the time cost and monetary cost. The time cost depends on the travel time on highways and the charging time while the monetary cost comes from the charging fare. We define a generalized travel cost (GTC) comprised of the travel time on the path, the charging time, and the charging fare to measure the total cost of a trip. The travel time is the total time consumption of traversing links on the network. The charging time/cost is assumed to have a fixed part and a charging amount-dependent part. The fixed time/cost of charging at type q station is denoted by

α_q / β_q while the time/cost per kWh is expressed by φ_q / λ_q. Both the travel time and the charging time are converted to the cost by a value-of-time denoted by υ.

2.3 Convex elastic demand function

In this study, it is assumed that the travelers could detour for battery charging and they are willing to travel on a deviation path if the GTC of that path is within a given threshold. Specifically, let C^w denote the minimum GTC of OD pair w and δ^w be the travelers' tolerance for the travel cost deviation. Then any travel path with a GTC within $\left(1+\delta^w\right)C^w$ is acceptable for the travelers of OD pair w. We further assume that the additional travel cost will cause the reduction of the travel demand and the traffic flows between each OD pair decline nonlinearly as the GTC increases. Let c^w be the GTC of OD pair w. Based on the logit-based form function proposed by Kim and Kuby (2012), we adopt the following function to depict the inverse relationship of the traffic flows between OD pair w and the GTC.

$$f^w\left(c^w\right) = F^w e^{-\theta^w\left(c^w - C^w\right)}, \quad \forall w \in W, C^w \le c^w \le \left(1+\delta^w\right)C^w \tag{1}$$

where F^w is the flow volume between OD pair w under the minimum travel cost C^w and θ^w denote travelers' sensitivity to the deviation of cost. A large θ^w implies a fast flow decay with the rise of GTC. The proposed log-based elastic demand function is convex and due to its favorable applicability, has been adopted by many transportation studies, e.g., Xu et al. (2018) and Yang and Huang (1997). We use an illustrative example (see Figure 1) to visualize the proposed elastic demand function. It is easy to find that the function performs a convex shape and that the traffic flows tend to be zero as the GTC goes to positive infinity.

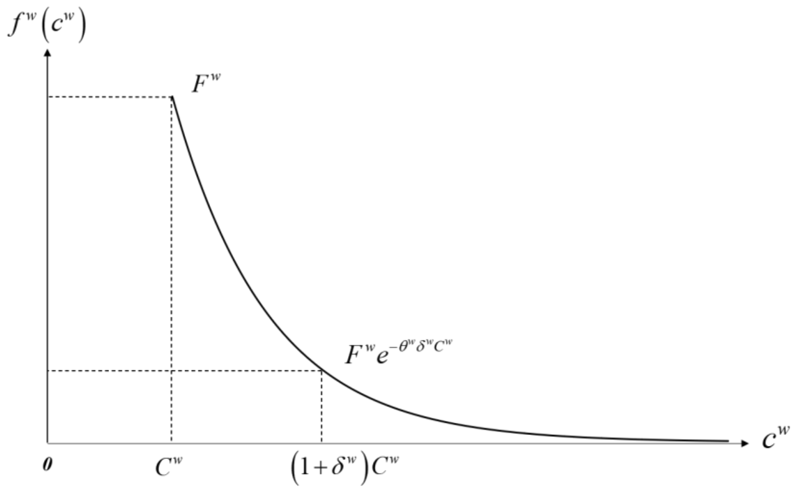

Figure 1 Variation of the traffic flows between OD pair w with the increase of GTC

The goal of the DMCS problem is to determine the optimal deployment of multi-type charging stations under budget B such that (i) the travelers drive along a cost acceptable travel path without battery depletion en-route and the final SOC is no less than E_D; (ii) the traffic flow between each OD pair follows the convex elastic demand function with respect to GTC; and (II) the total covered flows of all OD pairs are maximized.

3. A two-phase approach

This section elaborates on the two-phase solution method for the DMCS problem. Specifically, Subsection 3.1 formulates a mixed integer programming model to determine the most cost-saving path given a certain station deployment plan. Subsection 3.2 describes the procedure of initializing the deployment of charging stations. Subsection 3.3 illustrates the two-layer simulated annealing (TSA) algorithm for improving the quality of the incumbent deployment plans. Subsection 3.4 shows the solution acceleration strategy exploiting the high-quality deployment plans found by TSA.

3.1 Most cost-saving travel paths

Let us first illustrate the process of finding the optimal station deployment plan by the following steps to propose our two-phase approach. The first step is to construct a feasible station deployment plan subject to the given budget. The quality of the deployment plan in terms of the total covered flows will then be evaluated. By enumerating all possible station deployment plans, we can eventually obtain the optimal one. However, two issues should be carefully addressed when applying the above idea to solve the DMCS problem. First, since the number of feasible station deployment could be very large, enumerating all possible deployment plans seems impractical. Second, due to the nonlinear relationship of the covered flows and the GTC, using a nonlinear programming model to assess the covered flows could be computationally intensive. To apply the above idea, we need to (i) devise an intelligent rule of generating "promising" station deployments, and (ii) develop an efficient method to assess the covered flows under a given deployment plan. We will answer the second question in this subsection and respond to the first one in the next subsections.

Given the deployment of charging stations, intuitively, we should choose the most cost-saving travel path for the travelers in order to cover as many traffic flows as possible, which is in inverse proportion to the GTC. Herein, the most cost saving path of an OD pair refers to, under a given charging station deployment, the path that allows the drivers to complete their trips by the minimum travel cost. Such a kind of path is similar to the shortest path in some sense, except that we evaluate cost instead of path length. In other words, if we can find the most cost-saving path under the given deployment plan, the covered flows of each OD pair can be obtained by substituting the GTC into the convex elastic demand function. We formalize this idea by the following proposition:

Proposition 1. For a given station deployment plan, we will choose the most cost-saving travel path of each OD pair, referred to as MCTP, for the travelers such that the traffic flows are covered as many as possible.

Proof. We prove the proposition by contradiction. In particular, given a station deployment, suppose we have obtained the maximum covered flows under this deployment, while drivers of some OD pairs do not follow their most cost saving travel paths. Note that the elastic demand function is convex, and the covered flows monotonically decrease with the increase of travel cost. In this case, if the drivers, who originally travel on paths other than the most cost saving travel paths, now complete their trips by the most cost saving travel paths, their travel cost will decrease, and the covered flows will increase. This will contradict the assumption that we have found the maximum covered flows. Hence, all drivers will travel on the most cost saving paths to complete trips. □

The above proposition formally specifies the tight link between the drivers' optimal travel route and their minimum travel cost. With this finding ready, we are on the track of establishing the mechanism of our algorithm, that is iteratively generating deployment plans and meanwhile, improving the plan by assessing the covered flows.

To determine the MCTP under the given station deployment, we define the following decision variables for each OD pair: a binary variable $x_{ij}^{w}, \forall w \in W, (i, j) \in A$ representing whether link (i, j) is traversed by the path flow of OD pair w, and a binary variable $z^{w}, \forall w \in W$ denoting whether OD pair w is covered. Here, if an OD pair is covered, it means that the drivers of that OD pair are able to complete their travels under the given station deployment and importantly, the travel cost is within the prespecified threshold. The given station deployment is characterized by the station type at each candidate location. In this case, the charging cost-related parameters at a certain candidate location are known for us, allowing direct representation using index $s \in S$. The fixed time/cost and time/cost per kWh at a particular location s are denoted by α_s / β_s and φ_s / λ_s, respectively. With these variables, we propose a mixed-integer linear programming model, see Appendix 2, to determine the MCTP of OD pair w under a certain station deployment, referred to as the model [OP-I] for short thereafter.

If we maximize the covered flows between an OD pair under a given station deployment, we have to maximize the elastic demand function, leading to a nonlinear programming model. Instead, in Prop. 1 we find that the maximum covered flows are exactly the flows corresponding to the minimum travel cost. Hence, we can first find the minimum travel cost and then substitute this cost to the elastic demand function to obtain the covered flows. In this case, we directly minimize the travel cost and since the function of travel cost is linear, we are in fact solving MILP models. Specifically, the model [OP-I] minimizes GTC of OD pair w under a given station deployment. It returns the MCTP if OD pair w is covered under the available charging resources. We can then obtain the covered flows between OD pair w by substituting c^{w} into Eq. (1).

To conclude, leveraging the convexity of the elastic demand function and the inverse relationship of GTC and covered flows, we can obtain the covered flows by solving many small-scale mixed-integer linear programming models. Preliminary tests show that this model only needs, on average, about 0.01 s to find an MCTP on a mid-sized network. Its efficiency provides the potential of designing an iterative algorithm that gradually improves the quality of the station deployment plans according to the flow coverage.

3.2 Station deployment initialization

This subsection illustrates the station location initialization strategy according to the potential of each candidate location. The potential of each candidate location is obtained by solving the linear programming (LP) relaxation of the mixed-integer programming model proposed by Ouyang et al. (2020), see Appendix 3, which is referred to as the model [OP-II] for ease of representation.

Step 1: Solve the LP relaxation of the model [OP-II] under budget B and denote the solution value of the station location variables in the model [OP-II] by y_s^{fast} and $y_s^{slow}, \forall s \in S$, which originally represented whether a fast or a slow charging station is built at location s.

Step 2: Calculate the flows passing through each candidate location in the LP relaxation of the model [OP-II]. Denote the flows through location s by f_s.
Step 3: Use the following equation to evaluate the potential of each candidate location:

$$\tilde{f}_s = f_s\left(y_s^{slow} + \varpi_s y_s^{fast}\right), \quad \forall s \in S \tag{2}$$

where $\varpi_s = b_s^{fast} / b_s^{slow}$ is the cost ratio of building a fast and slow charging station at location s.
Step 4: Order all candidate locations in the descending order of their potential $\tilde{f}_s, \forall s \in S$. Denote the resultant location sequence by list $\mathcal{S}$.
Step 5: We construct different budget-feasible station deployment plans by adjusting the number of fast charging stations. Suppose we plan to allocate m fast charging stations on the network. Then these fast charging stations will be located at the first m locations in list $\mathcal{S}$. The remaining budget will be used to allocate slow charging stations from the $m+1$ location in list $\mathcal{S}$ one by one.
Step 6: Use the model [OP-I] and the elastic demand function to assess the covered flows of all deployments obtained in *Step 5*. Denote the incumbent best deployment plan, the largest flow coverage, and the flows passing through each candidate location by D^*, f^*, and $v_s^*, \forall s \in S$, respectively.

We supplement the following discussions as a remark. In Step 3, the potential of a candidate location is evaluated by Eq. (2). Imagine that we have known the optimal station deployment, then for a candidate location, its corresponding station type variable is either one or zero, meaning a type of station is located there or not. For a location chosen for building a station, there must be exactly one station type variable being one. “One” can be deemed that this location 100% contributes to the flows passing through it. In the LP relaxation model, a station type variable can be between zero and one. In this case, a location can be regarded to partially contribute to the flows passing through it. Let us look at Eq. (2) again. It represents the flows passing through a location weighted by the value of the station type variable. Since the construction costs of a slow and a fast charging station differ largely, we further introduce a cost ratio to strengthen the importance of the fast station type variable.

In Step 5, updating station deployments is rule-based. We can adjust the number of either fast or slow stations. In this study, we choose fast stations as the maximum number of building fast charging stations is smaller due to higher construction costs. In list $\mathcal{S}$, all candidate locations are sequenced in decreasing order of their potential. This suggests that the first location in the list could be the best choice to locate a fast charging station. Likewise, for the remaining location, their priorities of being chosen decline. Hence, we will choose the first m locations to build fast charging stations. After we have sited fast charging stations at the first m locations in the list $\mathcal{S}$, we will examine the remaining locations in decreasing order of their potential. In particular, if the left budget is sufficient to build a slow charging station at the examined location, then we build a slow charging station there; otherwise, we drop this location and examine the next location to see if we have enough money to build a slow charging station here. The above procedure will be conducted until we cannot build more stations.

3.3 Phase I: A two-layer simulated annealing heuristic

We find that once we fixed the station deployment, the total covered flows can be computed using the convexity of the objective function (as indicated in Prop. 1). We believe that there is no need to enumerate all possible station deployments as we could gradually improve the quality of the constructed deployment when more information (e.g., covered flows under different deployments) is available. This is a process of two steps and according to it, we devise a two-layer framework to improve the constructed deployment plans.

This subsection proposes a two-layer heuristic algorithm based on the simulated annealing (SA) framework to improve the quality of station deployment plans. The SA method is a well-known metaheuristic algorithm that iteratively generates feasible solutions and adjusts the solution generation rule based on the solution quality (Van Laarhoven and Aarts, 1987). A low-quality solution could be accepted to construct new solutions with some probability while the acceptance probability declines gradually, like an annealing process. This feature makes SA able to escape from the local optimum and possibly find the global optimum (Kirkpatrick et al., 1983). The SA has been extensively used in many transportation problems, e.g., Chiang and Russell (1996), Felipe et al. (2014), and Osman (1993).

In our heuristic, the outer layer generates a new station deployment plan based on the incumbent plan, and the deployment generation rule is refined according to the flows passing through each candidate location. To prevent the repeated appearance of the same low-quality station deployment plans, a Tabu list is embedded to store all poor deployment plans. The new deployment plan is then delivered to the inner layer and its covered flows are obtained via the model [OP-I] and the elastic demand function. The new deployment plan will replace the incumbent plan if it covers more flows or the flow gap of two deployments is smaller than a probabilistic threshold. Otherwise, the new deployment plan will be deemed to be a poor solution and is added to the Tabu list. The above operation is conducted iteratively until reaching the maximum iteration number. The procedure of the two-layer heuristic is summarized as follows:

Step 0: (Initialization) Set or initialize the annealing temperature T , the annealing ratio $\varepsilon \in (0,1)$, the poor location number k, the iteration index $l = 0$, the maximum iteration number L , the Tabu list $X_{Tabu} = \varnothing$, the best deployment plan D^*, the best flow coverage f^* , the incumbent deployment plan $\bar{D} = D^*$, the incumbent flow coverage $\bar{f} = f^*$, and the covered flows by each location $\bar{v}_s, \forall s \in S$.

Step 1: (Construct new deployment plan) Find the worst-k candidate locations according to $\bar{v}_s$ and randomly select one among these k locations. Denote the chosen location by $\tilde{s}$. Remove the station at location $\tilde{s}$ and use the construction cost of this station to allocate stations at other locations. Randomly select one of the following two strategies to locate new stations.

- *Strategy Fast*: Locate as many fast charging stations as possible and use the remaining budget to locate slow charging stations.
- *Strategy Slow*: Locate as many slow charging stations as possible and use the remaining budget to locate fast charging stations.

In both strategies, the priority of a location being chosen to build a charging station follows the decreasing order of $\bar{v}_s$. Check whether the new deployment plan is out of the Tabu list. If not, generate another deployment plan until it is not in the Tabu list. Denote the new deployment plan by D' . Note that since these two strategies aim to build as many fast/slow charging stations as possible, this could exhaust the budget and, in this case, we will not build slow/fast charging stations.

Step 2: (Assess the quality of the deployment plan) Use the model [OP-I] and the elastic demand function to obtain the flow coverage under the deployment plan D', denoted by f', and the flows through each location, denoted by $v'_s, \forall s \in S$.

Step 3: (Update the incumbent deployment plan and annealing temperature) If $f' > \bar{f}$, update the incumbent deployment plan, current flow coverage, and the flows through each location by $\bar{D} \leftarrow D'$, $\bar{f} \leftarrow f'$, and $\bar{v}_s \leftarrow v'_s, \forall s \in S$, respectively. If f' satisfies $e^{(f'-\bar{f})/T} \geq Rand(0,1)$, where the RHS is a randomly generated number between 0 and 1, update $\bar{D}$, $\bar{f}$, and $\bar{v}_s, \forall s \in S$ as well. Meanwhile, we reduce the annealing temperature by $T \leftarrow \varepsilon \cdot T$ so that a low-quality deployment plan becomes increasingly harder to replace the incumbent deployment plan in future iterations. If f' cannot satisfy either of the above conditions, we add this deployment plan into the Tabu list to ensure that such a deployment plan will not be delivered to the inner layer for the sake of time savings. Finally, update the iteration number by $l \leftarrow 1 + l$.
Step 4: (Update the best deployment plan) If $\bar{f} > f^*$, update the best deployment plan and the best flow coverage by $D^* \leftarrow \bar{D}$ and $f^* \leftarrow \bar{f}$, respectively.
Step 5: (Repeat the above steps) Repeat Step 1 to Step 4 until reaching the maximum iteration number, i.e., $l = L$.

The pseudo-code of the proposed TSA algorithm is presented in Appendix 4.

3.4 Phase II: Acceleration of solving the model [OP-II]

The first stage has identified some good station deployment plans. Still, we hope to further improve the solution quality or even find the optimal station deployment. We would like to resort to state-of-art MIP solvers in the second stage. To obtain the optimal station deployment, we use the best deployment plan found by the TSA heuristic as the initial solution for solving the model [OP-II] by MIP solvers. Assigning initial solution, especially a high-quality one, could help state-of-the-art MIP solvers, e.g., Gurobi, accelerate branch-and-bound as well as cut generation, thereby expediting the solving process. According to our experiment experience, assigning a good initial solution always helps accelerate solving the model. Thus, we introduce Phase-II in this study.

In this section, we use the best station deployment found in the first phase as the initial solution of the model [OP-II] to expedite solving the model [OP-II]. Note that at this stage, we are solving a MILP model. In Section 3.2, we solve the LP relaxation of the model [OP-II] to construct a station deployment. This deployment is then delivered to the two-layer heuristic algorithm to improve the deployment quality. Although Section 3.2 and 3.4 both use the model [OP-II], we are solving LP relaxation of [OP-II] and [OP-II], respectively. Likewise, although both introducing the notation "initialization", in Section 3.2 it represents the input for the two-layer heuristic, while in Section 3.4 it refers to the initial solution to [OP-II].

4. Case study and policy discussions

So far, an algorithm to find the optimal charging station deployment explicitly considering EV users' charging behavior has been established. Further, we will investigate its computational efficiency and how users' charging behavior, e.g., tolerance for travel cost deviation, and other external characteristics, e.g., total construction budget, impact the optimal station deployment. Moreover, to enhance promoting green transportation in the real world, we will derive various practical insights into policymaking in the context of Belt-and-Road Initiative (BRI). Briefly, this section aims to answer the following questions on the perspectives of both computation and application:

- Q1: Is the proposed two-phase approach able to solve the DMCS problem within a reasonable time? Which factors will affect the computational performance of the approach?
- Q2: Does allowing travel cost deviation affect governments' location planning and station operation? How about the influence of different tolerances for cost deviation on the station location?
- Q3: Can we derive some insightful suggestions for the governments involved in the BRI to devise their policy towards charging station location optimization and green transportation promotion?

To answer the above questions, we will use real-world data to perform extensive numerical experiments. The algorithm is coded in MATLAB 2020a calling GUROBI 9.0 and all tests are run on a personal desktop with a 3.2 GHz CUP and 16 GB memory.

4.1 Data description and algorithm settings

We use the real highway network of Zhejiang Province, China to perform the case study, which is a pioneering province to promote transport electrification promotion domestically. As of 2021, the provincial government plans to invest around RMB¥250 million in public charging facility construction (XinhuaNet, 2020). The highway network can be depicted by a directed graph consisting of 34 locations and 96 links (48 undirected links), see Figure 2. The length of each link is adopted from the database of the Zhejiang Provincial Department of Transportation. In the real world, the set of candidate locations is generally determined by the operator according to government policy and land availability. In our experiments, we assumed all 34 locations on the network can be chosen for building charging stations for simplicity. The EVs are assumed to be the second generation of NISSA LEAF that is equipped with a 40 kWh battery and a driving range of 243 km (Nissa, 2019). By assuming a constant speed of 120 km/hr and a constant battery discharging rate of 0.165 kWh/km, we can obtain the travel time and electricity consumption of each link. Following the convention of the facility location literature, the initial/final SOC of all EVs at origin/destination is required to be no more/less than half of the available battery capacity, i.e., 20 kWh. The construction cost of a fast/slow charging station at each candidate location is assumed to be 1/0.5 unit cost for simplicity. As for the charging activity-related parameters, we make the following settings: (a) the fixed time and charging time per kWh at a fast/slow charging station are 5 min/5 min and 0.6 min/2.2 min, respectively; (b) the fixed fare and charging fare per kWh at a fast/slow charging station are $2/$2 and $1/$0.5, respectively. All travelers' value-of-time is assumed to be $5/hr for convenience.

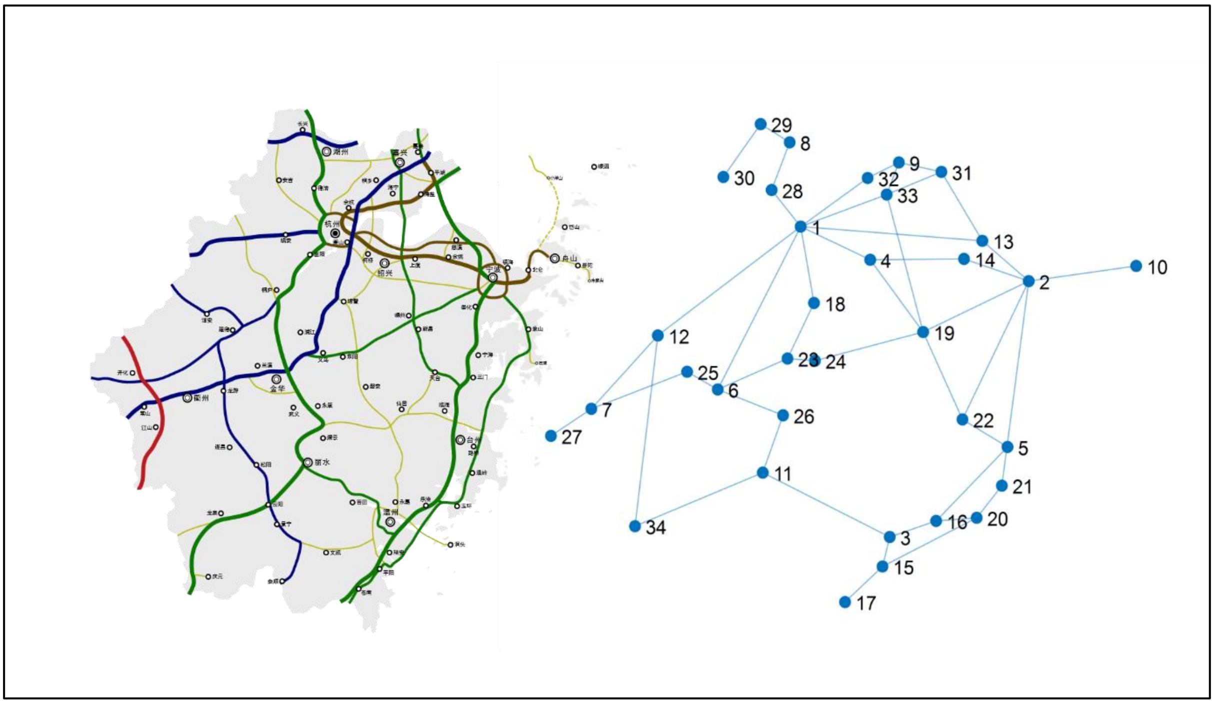

Figure 2 Highway network of Zhejiang Province, China.

To generate OD pairs, we choose the largest twenty cities of Zhejiang Province as the origin and destination, each of which has a population of over 1 million, and then obtain a total of 190 OD pairs. The gravity model (Hodgson, 1990) using the city population as weights is adopted to simulate the traffic flows between each OD pair, producing a total of 76708 flows. We drop the OD pairs of very small flow volume and eventually have 100 OD pairs with 72873 flows, which accounts for over 95% of all traffic flows. Regarding travelers' sensitivity to travel cost deviation, the parameters $\theta^w, \forall w \in W$ are calculated by assuming that the traffic flows of each OD pair will decrease to 20% of the maximum flow volume as the travel cost increases to 150% of the minimum travel cost.

Some preliminary tests are conducted to calibrate the parameters of the two-layer heuristic algorithm. The maximum number of iterations is limited to 25, which balances the time consumption and the solution quality. The number of low-quality locations that may be removed from the incumbent station deployment is set to be 3. This setting controls the number of possible new deployments in a suitable size. The initial annealing temperature and the annealing ratio are set to be 3000 and 0.98 respectively, which makes the annealing process progresses at a moderate rate. We do not restrict the size of the Tabu list, suggesting that all station layout deemed as a low-quality result by the heuristic algorithm will be recorded and will not be delivered into the inner layer for the sake of time saving. The total runtime limitation of the heuristic is set to be 60 sec while the solver runtime in the second stage is limited to 10,800 sec. The time limit for directly solving the model [OP-II] by GUROBI is also limited to 10,800 sec.

4.2 Algorithm performance analysis and comparative study

One of the contributions of this study is the two-phase approach to the DMCS problem. In this section, we will assess the performance of the approach by extensive experiments and further compare its efficiency with the existing method. To this end, we will compare the runtime of two methods consumed by finding the optimal solution. If we use less time, then we win. For large-scale test instances that the existing method is unable to find the optimal solution within an acceptable time (3 hours), we record the optimality gaps when given time is exhausted and then run our approach to attain the same gaps. If our approach uses much less time, we believe we outperform the existing method considerably.

To assess the algorithm performance under different parameter settings, we generate a total of 80 test instances by varying the budget between $\{1, 2, 3, \ldots, 20\}$ and letting tolerance for cost deviation equaling to $\{0, 0.1, 0.2, 0.3\}$. The variable budget and tolerance can be regarded as simulating different financial policies and green transportation acceptance. We report the computational time required by our approach and the model [OP-II] on these 80 instances in Table 1. The columns named by [OP-II], Phase I, and Phase II record the time of directly solving the model [OP-II] via GUROBI, the runtime of Phase I and Phase II, respectively. Kindly note that in 12 test instances, the model [OP-II] cannot be directly solved to optimality by the solver within 10,800 sec, which is highlighted by italics. We report the relative gap - (best upper bound – best objective value)/ best objective value - when the solver terminates for each instance in the column named by Gap. For comparison, the time required by our approach for achieving the same gap is presented in the column Phase II for these 12 instances. The saved time of the two-phase approach, i.e., Phase I + Phase II – [OP-II], is listed in the column Saving.

Figure 3 shows the runtime of the heuristic algorithm under four different tolerance levels for travel cost deviation as budget increases from 1 to 20. It can be seen that under any budget and tolerance level, the algorithm can complete 25 iterations within 45 sec. In more than 60% of the test instances, the average runtime of an iteration does not exceed 1 sec. These results demonstrate the efficiency of the heuristic algorithm, which can be attributed to the merits of the model [OP-I] that can determine the MCTP for each OD pair quickly. Clearly, with more budget available, the runtime performs an upward trend no matter tolerance levels. This may be explained by that more open charging stations make the network more complex and thus the model [OP-I] needs a longer time to find the MCTP of an OD pair. In addition, allowing a larger value of tolerance could also call for more computational time. For example, the runtime under the tolerance of 0.3 surges after the budget exceeds 11. This observation is consistent with our expectation that a bigger tolerance would make finding the MCTP harder. It is, however, worthwhile to note that the exact impact of tolerance and budget on runtime is unclear since in fact, given a tolerance level, the runtime fluctuates with the growth of budget, and fixing the budget, the runtime under a higher tolerance could be smaller than that under a lower tolerance.

Table 1 Comparison of the computation time of the proposed two-phase approach and directly solving the model [OP-II].

B	Tolerance 0				Tolerance 0.1				Tolerance 0.2					Tolerance 0.3				
	[OP-II]	Phase I	Phase II	Saving	[OP-II]	Phase I	Phase II	Saving	[OP-II]	Gap	Phase I	Phase II	Saving	[OP-II]	Gap	Phase I	Phase II	Saving
2	7	14	5	-13	15	13	16	-14	32	/	15	21	-5	38	/	13	36	-11
4	12	12	12	-12	28	15	25	-11	83	/	13	43	27	116	/	13	99	4
6	38	13	33	-8	100	15	72	13	361	/	16	275	70	371	/	15	361	-5
8	45	12	44	-11	179	14	160	5	1,498	/	14	636	848	1,232	/	17	1,112	103
10	53	14	46	-7	817	17	645	155	2,089	/	20	1,703	366	*10,800*	*0.003*	21	*9,359*	*1,420*
12	54	17	52	-16	434	17	236	181	3,602	/	18	1,879	1,705	*10,800*	*0.006*	18	*4,602*	*6,180*
14	53	19	50	-16	714	20	618	75	4,450	/	18	3,666	766	*10,800*	*0.005*	19	*7,905*	*2,876*
16	92	19	60	13	546	18	441	86	*10,800*	*0.002*	19	*6,309*	*4,472*	*10,800*	*0.006*	20	*5,757*	*5,023*
18	156	23	105	28	720	21	520	178	9,045	/	23	5,528	3,495	*10,800*	*0.012*	20	*9,631*	*1,149*
20	168	21	125	22	488	22	407	59	*10,800*	*0.002*	24	*9,573*	*1,203*	*10,800*	*0.014*	25	*5,019*	*5,756*
22	107	22	81	4	685	25	644	16	*10,800*	*0.003*	25	*4,418*	*6,357*	*10,800*	*0.008*	24	*8,248*	*2,528*
24	286	25	97	164	1,225	25	528	673	*10,800*	*0.002*	29	*6,454*	*4,317*	*10,800*	*0.004*	35	*7,447*	*3,318*
26	189	27	65	97	395	26	206	162	3,120	/	28	2,214	879	2,509	/	38	1,665	806
28	44	28	36	-20	226	27	113	85	1,097	/	28	322	747	1,250	/	41	1,203	6
30	55	24	33	-2	192	28	61	103	397	/	31	222	144	975	/	37	956	-18
32	60	26	50	-15	194	30	72	92	177	/	26	170	-19	344	/	41	305	-2
34	76	26	65	-15	85	27	68	-11	144	/	29	123	-8	226	/	38	203	-15
36	65	27	53	-15	89	25	12	53	140	/	29	14	97	74	/	41	16	17
38	61	28	23	10	30	25	9	-4	65	/	28	8	29	62	/	42	19	1
40	34	29	20	-15	21	25	8	-12	57	/	29	11	17	34	/	45	19	-30

Remark: The elapsed time of each test instance is measured in sec. We cannot directly solve the model [OP-II] to optimality within 10,800 sec in 12 instances, which are marked in italics; the relative gap of 12 instances returned by the solver are reported. For comparison, we display the time required in Phase II to reach the same relative gap in these 12 instances.

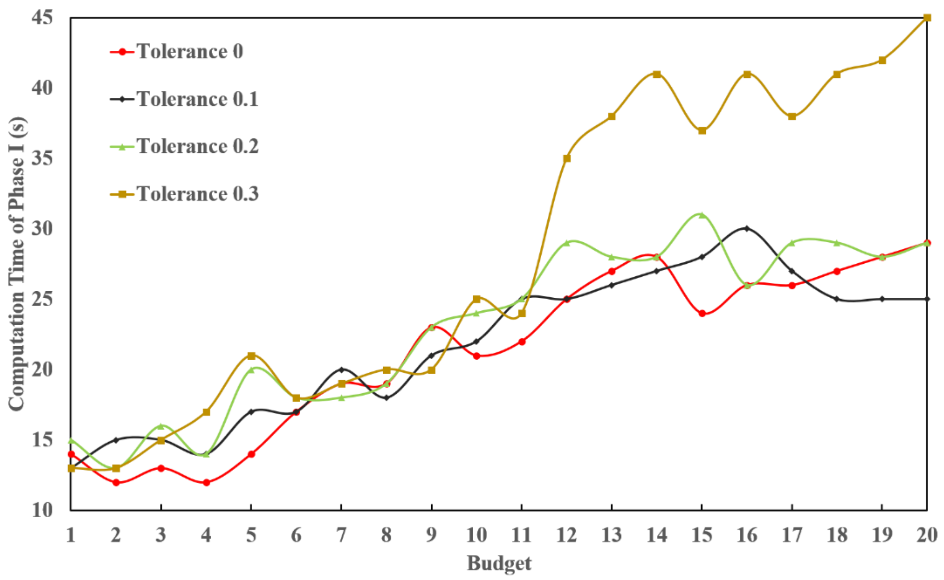

Figure 3 Variations of the runtime of Phase I with the increase of budget under different tolerance.

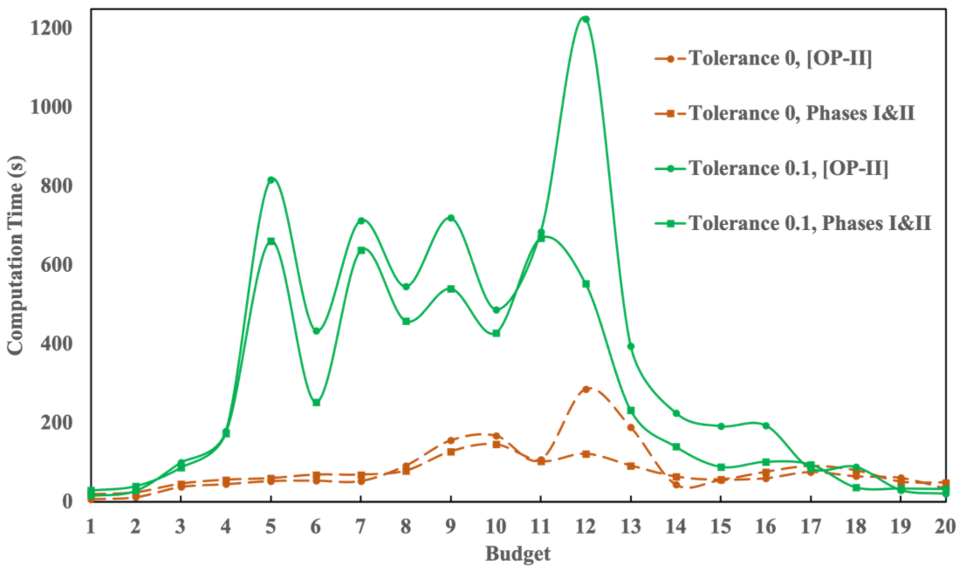

Figure 4 Variations of the runtime of the two-phase approach and the model [OP-II] with the increase of budget under different travel cost deviation tolerances.

We further visualize the total runtime of our two-phase approach under the tolerance of 0 and 0.1 in comparison with the time required for directly solving the model [OP-II] in Figure 4. It is easy to find that allowing a higher tolerance level leads both our approach and the model [OP-II], by and large, to use more time. Regarding the impact of budget on the algorithm performance, the runtime shows a mountain shape. Specifically, take tolerance of 0.1 for example, first witnessing a constant rise as budget increases from 1 to 5, the runtime then performs a significant fluctuation when the budget varies between 6 and 12, followed by a jump after over 13 unit costs are available. Besides, for both tolerance levels, the most time-consuming cases always occur when the budget equals 12. Under tolerance of 0.1, almost in all test instances, our approach consumes less time, and the largest time saving is up to 673 sec. However, when the cost deviation is forbidden, directly solving the model [OP-II] can be slightly more efficient in some instances. This is because that the model [OP-II] is already readily solvable if tolerance equals zero, whereas our approach needs additional time in Phase I. Fortunately, our approach significantly outperforms when higher tolerance levels are considered because the rising tolerance results in the exponential increase of directly solving the model [OP-II] and the merits of adopting a high-quality initial solution becomes obvious. For instance, with a tolerance of 0.2 and 0.3, the maximum time savings are 6357 sec and 6180 sec, respectively. The above results suggest the efficacy of our two-phase approach, especially under hard parameter settings such as a high tolerance for cost deviation.

4.3 Policy discussion

4.3.1 Understanding travelers' travel cost deviation tolerance

Table 2 tabulates the covered flow volume and the number of covered OD pairs under the tolerance of 0, 0.1, 0.2, and 0.3 as we increase the budget from 1 to 20 one by one. For ease of discussion, we further visualize the ratios of the covered flow volume and covered OD pairs as budget increases in Figure 5 and Figure 6, respectively. It can be seen that under any of the four tolerances, following a quick rise before budget exceeds 4, the ratio of the covered flow volume then increases with a near-linear rate, followed by a slower and slower increase after more than 13 unit costs are available, making the entire increase curve have a near concave shape. It is worthwhile to note that no matter how much budget is given, the covered flow volume under a high tolerance is always greater than that under a low tolerance, which is in line with our expectation that a larger tolerance allows more flexible charging options, thereby attracting more travelers.

Table 2 Comparison of the covered flows and covered OD pairs under different cost deviation tolerances.

B	Tolerance 0		Tolerance 0.1		Tolerance 0.2		Tolerance 0.3	
	No. Flows	No. Pairs	No. Flows	No. Pairs	No. Flows	No. Pairs	No. Flows	No. Pairs
1	12,987	2	12,987	2	12,987	2	12,987	2
2	20,914	6	22,459	10	22,685	11	22,685	11
3	26,167	10	28,283	12	29,771	17	29,771	17
4	30,959	13	33,618	15	35,928	27	36,630	30
5	35,358	17	37,759	28	39,917	35	40,956	42
6	39,736	19	43,023	28	45,411	45	46,282	49
7	45,113	26	48,902	45	50,971	59	51,970	65
8	49,352	34	53,609	55	56,322	68	57,030	71
9	52,816	46	57,264	63	59,722	72	60,495	84
10	56,928	57	61,008	71	62,830	83	64,134	93
11	60,416	63	64,037	76	66,048	93	66,991	98
12	63,393	71	67,320	90	68,537	94	69,487	99
13	66,756	80	70,409	96	70,696	98	71,245	100
14	69,640	87	72,096	99	72,176	100	72,357	100
15	70,603	89	72,640	100	72,640	100	72,640	100
16	71,280	92	72,727	100	72,727	100	72,727	100
17	71,963	95	72,773	100	72,773	100	72,773	100
18	72,389	98	72,801	100	72,807	100	72,807	100
19	72,681	99	72,836	100	72,854	100	72,854	100
20	72,873	100	72,873	100	72,873	100	72,873	100

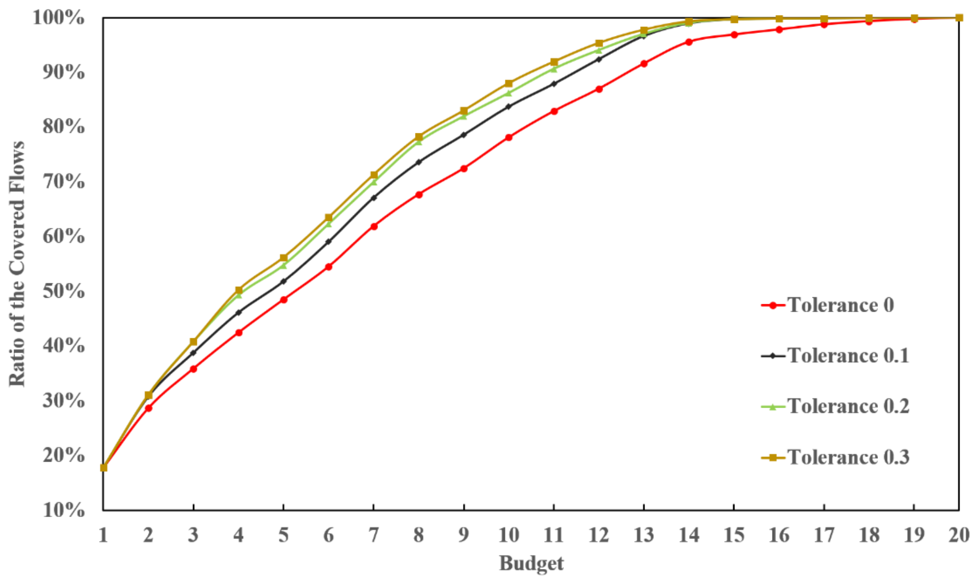

Figure 5 Variations of the ratio of the covered flows with the increase of budget under different cost deviation tolerances.

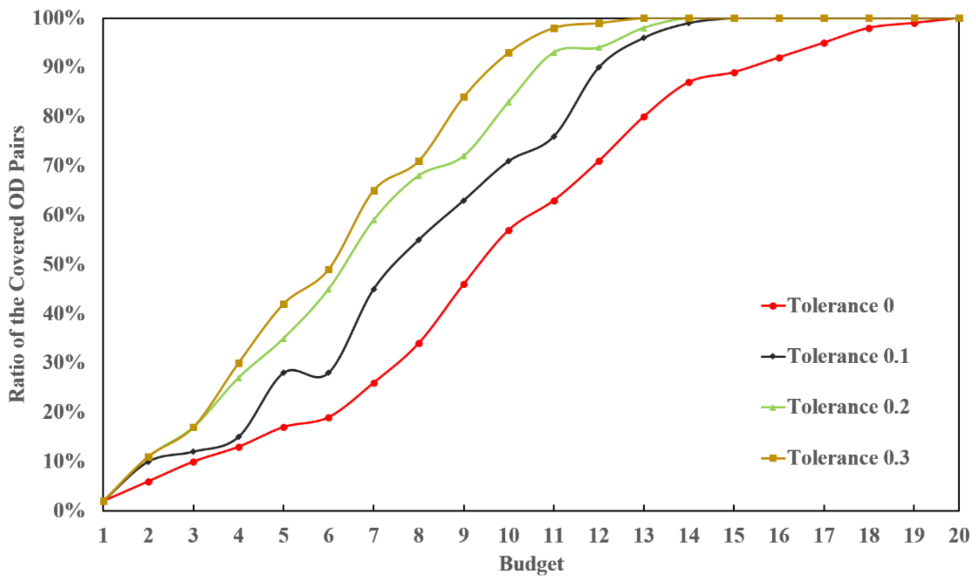

Figure 6 Variations of the ratio of the covered OD pairs with the increase of budget under different cost deviation tolerances.

As shown in Fig. 7, similar to the impact of budget on the covered flow volume, the ratio of covered OD pairs generally rises with the increase of budget. However, the increase in the ratio is not stable. For example, the ratio hardly changes as the budget rises from 5 to 6 under the tolerance of 0.1. For another example, when the travelers accept an additional 20% of the minimum travel cost, increasing the budget from 11 to 12 does not contribute to the ratio increase. Also, like the influence of tolerance on the covered flow volume, a large tolerance leads to a higher ratio of the covered OD pairs. These observations motivate us to design the charging station location policy combing with the practical condition of a country.

Before devising a charging station location strategy, the government is expected to fully understand the user's tolerance for travel cost deviations. Through the above experimental results, we can find that if the user has a higher tolerance, the same level of the flow coverage can be achieved with less investment. To obtain consumers' tolerance for travel cost deviation, the government can conduct questionnaires, surveys, and interviews with EV users and can also expand the surveyed travelers to potential buyers of EVs. Some state-of-art techniques, such as machine learning, can be adopted to analyze travelers' feedbacks so as to obtain more reliable tolerance values. Accepting travel cost deviation means that the travelers are willing to adopt EVs as their transport modes even if they need to pay additional travel costs resulting from the scarce charging resources. The additional cost paid by the travelers can be regarded as a subsidiary to the local government's limited budget. In the developed countries in the BRI, particularly where transportation is popularized such as European countries, the travelers may be more supportive of environmentally friendly and sustainable transport modes and are more willing to choose EVs. By contrast, in some developing countries in the BRI such as African countries, people may be unwilling to pay extra costs for using EVs. Therefore, for countries with insufficient funds, it is particularly important to increase people's awareness of green travel. Through advertising the merits of green transportation, people may gradually accept a higher cost deviation, which helps the charging stations serve more charging demands under the limited budget. To enhance people's awareness of green travel, the government may distribute promotional materials in communities, schools, and gasoline supply stations and may also provide subsidies to charging stations to reduce EV users' charging costs.

4.3.2 Budget policy suggestions

Since the participants of the BRI have different economic levels, their budget policy towards promoting transport electrification may be distinct to each other. For some developed countries, the government may have sufficient budget to implement large-scale charging station construction; while for some developing countries, the government's budget may be only enough to build a few amounts of stations. In this section, we try to give some practical suggestions on how to devise budget policies on building charging stations for countries with different levels of economic development. To understand the impact of budget on the charging demand fulfillment, we calculate the marginal utility of the available budget with respect to the covered flow volume and the covered OD pairs under the tolerance of 0, 0.1, 0.2, and 0.3. In Table 3, the columns named by MU. Flows and MU. Pairs represent the increased ratios of covered flows and OD pairs when we provide an additional 1 unit cost compared with the budget listed in the first column. It can be found that as more budget available, the marginal utility of budget with respect to the flow coverage constantly declines; while the marginal utility of budget with respect to the covered OD pairs fluctuates and does not perform a certain obvious pattern.

Table 3 Comparison of the marginal utility of budget under different cost deviation tolerances.

B	Tolerance 0		Tolerance 0.1		Tolerance 0.2		Tolerance 0.3	
	MU. Flows	MU. Pairs	MU. Flows	MU. Pairs	MU. Flows	MU. Pairs	MU. Flows	MU. Pairs
0	0.178	0.020	0.178	0.020	0.178	0.020	0.178	0.020
1	0.109	0.040	0.130	0.080	0.133	0.090	0.133	0.090
2	0.072	0.040	0.080	0.020	0.097	0.060	0.097	0.060
3	0.066	0.030	0.073	0.030	0.084	0.100	0.094	0.130

4	0.060	0.040	0.057	0.130	0.055	0.080	0.059	0.120
5	0.060	0.020	0.072	0.000	0.075	0.100	0.073	0.070
6	0.074	0.070	0.081	0.170	0.076	0.140	0.078	0.160
7	0.058	0.080	0.065	0.100	0.073	0.090	0.069	0.060
8	0.048	0.120	0.050	0.080	0.047	0.040	0.048	0.130
9	0.056	0.110	0.051	0.080	0.043	0.110	0.050	0.090
10	0.048	0.060	0.042	0.050	0.044	0.100	0.039	0.050
11	0.041	0.080	0.045	0.140	0.034	0.010	0.034	0.010
12	0.046	0.090	0.042	0.060	0.030	0.040	0.024	0.010
13	0.040	0.070	0.023	0.030	0.020	0.020	0.015	0.000
14	0.013	0.020	0.007	0.010	0.006	0.000	0.004	0.000
15	0.009	0.030	0.001	0.000	0.001	0.000	0.001	0.000
16	0.009	0.030	0.001	0.000	0.001	0.000	0.001	0.000
17	0.006	0.030	0.000	0.000	0.000	0.000	0.000	0.000
18	0.004	0.010	0.000	0.000	0.001	0.000	0.001	0.000
19	0.003	0.010	0.001	0.000	0.000	0.000	0.000	0.000

It is worth noting that under the tolerance of 0.3, all OD pairs can be covered with a budget of 12 while the ratio of the covered flow volume is around 95%, meaning that further increasing budget does not cover more travel routes but reduces the travel cost through providing more efficient charging service. With more budget for building more fast charging stations, the EV users can travel along a more cost-saving travel path, which attracts more travelers to use EVs for traveling. When the budget reaches a certain value, all OD pairs have been covered and the government often needs to invest a lot of additional budget to improve the flow coverage. For example, intending to cover 95% of all flows, the government needs to invest 13, 12, 12, and 11 unit costs under the tolerance of 0, 0.1, 0.2, and 0.3, respectively; however, to attain the 100% flow coverage, additional 7, 8, 8, and 9 unit costs are required, respectively. Therefore, for countries with insufficient budget, we do not recommend the government to invest too much in building charging stations. On the contrary, we recommend a more economical budget policy that uses a limited budget to achieve acceptable flow coverage. In addition, even for countries with ample budget, it may be better to cover 95% of all flows since serving the remaining 5% flows needs a huge amount of investment, which is uneconomical.

4.3.3 Station type and location suggestions

Table 4 and Table 5 tabulate the locations chosen for being allocated charging stations under four tolerance levels and a different budget. It can be found that the station type at a certain location is influenced by the value of tolerance. For example, given 8 unit costs available for building stations and any cost deviation being unacceptable, the only fast charging station is placed at location 14; as tolerance rises to 0.1, all 8 unit costs are used to install slow charging stations. For another example, under the budget of 12 and tolerance of 0.2, we construct fast charging stations at locations 2, 4, and 16; in contrast, if tolerance is 0.3, only locations 2 and 16 are installed with fast charging stations while the extra budget is put into slow charging station construction. This phenomenon may be explained by that when tolerance gets increased, users could detour to a far station for battery charging and the model would tend to allocate more economical slow charging stations so as to cover more OD travel paths. Additionally, it is worth noting that some locations are placed charging stations under almost all budget and tolerance levels, such as locations 1, 3, 14, and 15. These stations are all big cites in Zhejiang, which are also the origins or destinations of OD pairs with large flow volumes. The results are consistent with the practical experience of prioritizing to build charging stations in big cities. On the other hand,

Table 4 Station location comparison under the tolerance of 0 and 0.1 with the increase of budget.

B	Tolerance 0		Tolerance 0.1	
	Fast Station No.	Slow Station No.	Fast Station No.	Slow Station No.
2	/	4, 15	/	4, 15
4	/	4, 9, 15, 16	/	4, 14, 15, 16
6	/	4, 9, 14, 15, 16, 22	/	4, 9, 14, 15, 16, 22
8	14	4, 9, 13, 15, 16, 22	/	4, 5, 9, 13, 14, 15, 16, 22
10	2, 16	4, 5, 9, 14, 15, 22	2, 5	4, 9, 13, 15, 16, 22
12	1, 2, 16	4, 5, 9, 13, 15, 22	1, 2	4, 5, 9, 13, 14, 15, 16, 22
14	1, 2, 16	4, 5, 8, 9, 13, 14, 15, 22	1, 2, 5	4, 8, 9, 13, 14, 15, 16, 22
16	1, 2, 16	4, 5, 8, 9, 13, 14, 15, 18, 22, 23	1, 2, 5	4, 8, 9, 13, 14, 15, 16, 18, 22, 23
18	1, 2, 16, 22	4, 5, 8, 9, 13, 14, 15, 18, 21, 23	1, 2, 5	4, 8, 9, 13, 14, 15, 16, 17, 18, 21, 22, 23
20	1, 2, 16, 19, 22	4, 5, 6, 8, 9, 13, 14, 15, 21, 23	1, 2, 5, 19	4, 6, 8, 9, 13, 14, 15, 16, 18, 21, 22, 23
22	1, 2, 16, 19, 22	4, 5, 6, 8, 9, 13, 14, 15, 17, 18, 21, 23	1, 2, 5, 19	4, 6, 8, 9, 10, 13, 14, 15, 16, 17, 18, 21, 22, 23
24	1, 2, 3, 5, 6, 19	4, 8, 9, 11, 13, 14, 15, 16, 18, 21, 22, 23	1, 2, 3, 5, 6, 19	4, 8, 9, 11, 13, 14, 15, 16, 18, 21, 22, 23
26	1, 2, 3, 5, 6, 11, 19	4, 8, 9, 13, 14, 15, 16, 17, 18, 21, 22, 23	1, 2, 3, 5, 6, 19	4, 7, 8, 9, 11, 13, 14, 15, 16, 17, 18, 21, 22, 23
28	1, 2, 3, 5, 6, 11, 19	4, 7, 8, 9, 10, 13, 14, 15, 16, 17, 18, 21, 22, 23	1, 2, 3, 5, 6, 19	4, 7, 8, 9, 10, 11, 12, 13, 14, 15, 16, 17, 18, 21, 22, 23
30	1, 2, 3, 5, 6, 18, 19, 26	4, 7, 8, 9, 10, 11, 13, 14, 15, 16, 17, 21, 22, 23	1, 2, 3, 5, 6, 11, 12, 19	4, 7, 8, 9, 10, 13, 14, 15, 16, 17, 18, 21, 22, 23
32	1, 2, 3, 5, 6, 9, 18, 19, 22, 26	4, 7, 8, 10, 11, 13, 14, 15, 16, 17, 21, 23	1, 2, 3, 4, 5, 6, 9, 11, 12, 19	7, 8, 10, 13, 14, 15, 16, 17, 18, 21, 22, 23
34	1, 2, 3, 5, 6, 9, 12, 18, 19, 22, 26	4, 7, 8, 10, 11, 13, 14, 15, 16, 17, 21, 23	1, 2, 3, 4, 5, 6, 9, 11, 12, 19, 28	7, 8, 10, 13, 14, 15, 16, 17, 18, 21, 22, 23
36	1, 2, 3, 5, 6, 9, 11, 12, 13, 18, 19, 22, 26	4, 7, 8, 10, 14, 15, 16, 17, 21, 23	1, 2, 3, 4, 5, 6, 9, 11, 12, 13, 19, 22, 28	7, 8, 10, 14, 15, 16, 17, 18, 21, 23
38	1, 2, 3, 4, 5, 6, 9, 11, 12, 18, 19, 22, 26, 28	7, 8, 10, 13, 14, 15, 16, 17, 21, 23	1, 2, 3, 4, 5, 6, 9, 11, 12, 18, 19, 22, 26, 28	7, 8, 10, 13, 14, 15, 16, 17, 21, 23
40	1, 2, 3, 4, 5, 6, 9, 11, 12, 13, 16, 18, 19, 22, 26, 28	7, 8, 10, 14, 15, 17, 21, 23	1, 2, 3, 4, 5, 6, 9, 11, 12, 13, 15, 19, 22, 23, 26, 28	7, 8, 10, 14, 16, 17, 18, 21

Table 5 Station location comparison under the tolerance of 0.2 and 0.3 with the increase of budget.

B	Tolerance 0.2		Tolerance 0.3	
	Fast Station No.	Slow Station No.	Fast Station No.	Slow Station No.
2	/	4, 15	/	4, 15
4	/	4, 14, 15, 16	/	4, 14, 15, 16
6	/	4, 9, 13, 14, 15, 16	/	4, 9, 13, 14, 15, 16
8	16	4, 9, 13, 14, 15, 22	16	4, 9, 13, 14, 15, 22
10	16	4, 9, 13, 14, 15, 18, 22, 23	16	4, 9, 13, 14, 15, 18, 22, 23
12	2, 4, 16	5, 9, 13, 14, 15, 22	2, 16	1, 4, 5, 9, 13, 14, 15, 22
14	1, 2, 16	4, 5, 8, 9, 13, 15, 22, 23	1, 2, 16	4, 5, 8, 9, 13, 15, 22, 23
16	1, 2, 16	4, 5, 6, 8, 9, 13, 14, 15, 22, 23	1, 2, 16	4, 5, 6, 8, 9, 13, 14, 15, 22, 23
18	1, 2, 16	4, 5, 6, 8, 9, 13, 14, 15, 17, 18, 22, 23	1, 2, 16	4, 5, 6, 8, 9, 11, 13, 14, 15, 18, 22, 23
20	1, 2, 3	4, 5, 6, 8, 9, 11, 13, 14, 15, 16, 18, 21, 22, 23	1, 2, 3, 6	4, 5, 8, 9, 11, 13, 14, 15, 16, 18, 22, 23
22	1, 2, 3, 6	4, 5, 8, 9, 11, 13, 14, 15, 16, 17, 18, 21, 22, 23	1, 2, 3, 6	4, 5, 8, 9, 11, 13, 14, 15, 16, 17, 18, 21, 22, 23
24	1, 2, 3, 5, 6	4, 8, 9, 10, 11, 13, 14, 15, 16, 17, 18, 21, 22, 23	1, 2, 3, 5, 6	4, 8, 9, 10, 11, 13, 14, 15, 16, 17, 18, 21, 22, 23
26	1, 2, 3, 5, 6, 19	4, 8, 9, 10, 11, 13, 14, 15, 16, 17, 18, 21, 22, 23	1, 2, 3, 5, 6, 19	4, 8, 9, 10, 11, 13, 14, 15, 16, 17, 18, 21, 22, 23
28	1, 2, 3, 5, 6, 19	4, 7, 8, 9, 10, 11, 12, 13, 14, 15, 16, 17, 18, 21, 22, 23	1, 2, 3, 5, 6, 11, 19	4, 7, 8, 9, 10, 13, 14, 15, 16, 17, 18, 21, 22, 23
30	1, 2, 3, 5, 6, 11, 12, 19	4, 7, 8, 9, 10, 13, 14, 15, 16, 17, 18, 21, 22, 23	1, 2, 3, 5, 6, 11, 12, 19	4, 7, 8, 9, 10, 13, 14, 15, 16, 17, 18, 21, 22, 23
32	1, 2, 3, 4, 5, 6, 9, 11, 12, 19	7, 8, 10, 13, 14, 15, 16, 17, 18, 21, 22, 23	1, 2, 3, 4, 5, 6, 9, 11, 12, 19	7, 8, 10, 13, 14, 15, 16, 17, 18, 21, 22, 23
34	1, 2, 3, 4, 5, 6, 9, 11, 12, 19, 28	7, 8, 10, 13, 14, 15, 16, 17, 18, 21, 22, 23	1, 2, 3, 4, 5, 6, 9, 11, 12, 19, 28	7, 8, 10, 13, 14, 15, 16, 17, 18, 21, 22, 23
36	1, 2, 3, 4, 5, 6, 9, 11, 12, 13, 19, 22, 28	7, 8, 10, 14, 15, 16, 17, 18, 21, 23	1, 2, 3, 4, 5, 6, 9, 11, 12, 13, 19, 22, 28	7, 8, 10, 14, 15, 16, 17, 18, 21, 23
38	1, 2, 3, 4, 5, 6, 9, 11, 12, 18, 19, 22, 26, 28	7, 8, 10, 13, 14, 15, 16, 17, 21, 23	1, 2, 3, 4, 5, 6, 9, 11, 12, 18, 19, 22, 26, 28	7, 8, 10, 13, 14, 15, 16, 17, 21, 23
40	1, 2, 3, 4, 5, 6, 7, 9, 11, 12, 13, 18, 19, 22, 26, 28	8, 10, 14, 15, 16, 17, 21, 23	1, 2, 3, 4, 5, 6, 9, 11, 12, 13, 16, 18, 19, 22, 26, 28	7, 8, 10, 14, 15, 17, 21, 23

some locations have never been placed charging stations, such as locations 29, 30, 31, 32, 33, and 34, which are all small cities with less than one million population.

Table 6 reports in detail the number of two types of stations under different budgets and tolerances. We further visualize the variations of the number of stations with the increase of budget in Figure 7 for sake of discussion. It can be seen that under four tolerance levels, the number of fast charging stations witnesses a steady increase with the growth of budget whereas the number of slow charging stations, by and large, first rises and then declines after the budget exceeds 14, performing a mountain shape. Interestingly, under the tolerance of 0.1 and 0.2, the number of slow charging stations fluctuates as the budget varies between 4 and 12. For instance, when tolerance is 0.1, the number of slow charging stations decreases from 8 to 6 as the budget rises from 4 to 5; also, the number becomes from 14 to 12 when an additional one unit cost is available compared with the budget of 11. Besides, under each of the four tolerances, the number of fast charging stations surpasses that of slow charging stations after the budget exceeds 35. Different from the intuition of placing more fast charging stations, the experimental results tell us that in most cases, the government should build more slow charging stations to cover more travel paths, instead of prioritizing fast station construction for improving charging efficiency. Some developing countries in the BRI may not have enough budget to conduct large-scale charging station construction and may also not have a compatible power grid supporting fast charging station operations. In this case, the government is supposed to first build slow charging stations to refuel as many travel routes as possible and then to consider improving the charging efficiency. Fortunately, we can see, as shown in the previous section, that even with a very limited budget, we can success to over 90% of all flows under any tolerance level. This observation consolidates the policy that prioritizes building stations at the early stage of promoting transport electrification.

Table 6 Comparison of the number of charging stations with the increase of budget under different cost deviation tolerances.

B	Tolerance 0		Tolerance 0.1		Tolerance 0.2		Tolerance 0.3	
	No. Fast	No. Slow	No. Fast	No. Slow	No. Fast	No. Slow	No. Fast	No. Slow
1	0	2	0	2	0	2	0	2
2	0	4	0	4	0	4	0	4
3	0	6	0	6	0	6	0	6
4	1	6	0	8	1	6	1	6
5	2	6	2	6	1	8	1	8
6	3	6	2	8	3	6	2	8
7	3	8	3	8	3	8	3	8
8	3	10	3	10	3	10	3	10
9	4	10	3	12	3	12	3	12
10	5	10	4	12	3	14	4	12
11	5	12	4	14	4	14	4	14
12	6	12	6	12	5	14	5	14
13	7	12	6	14	6	14	6	14
14	7	14	6	16	6	16	7	14
15	8	14	8	14	8	14	8	14
16	10	12	10	12	10	12	10	12
17	11	12	11	12	11	12	11	12
18	13	10	13	10	13	10	13	10
19	14	10	14	10	14	10	14	10
20	16	8	16	8	16	8	16	8

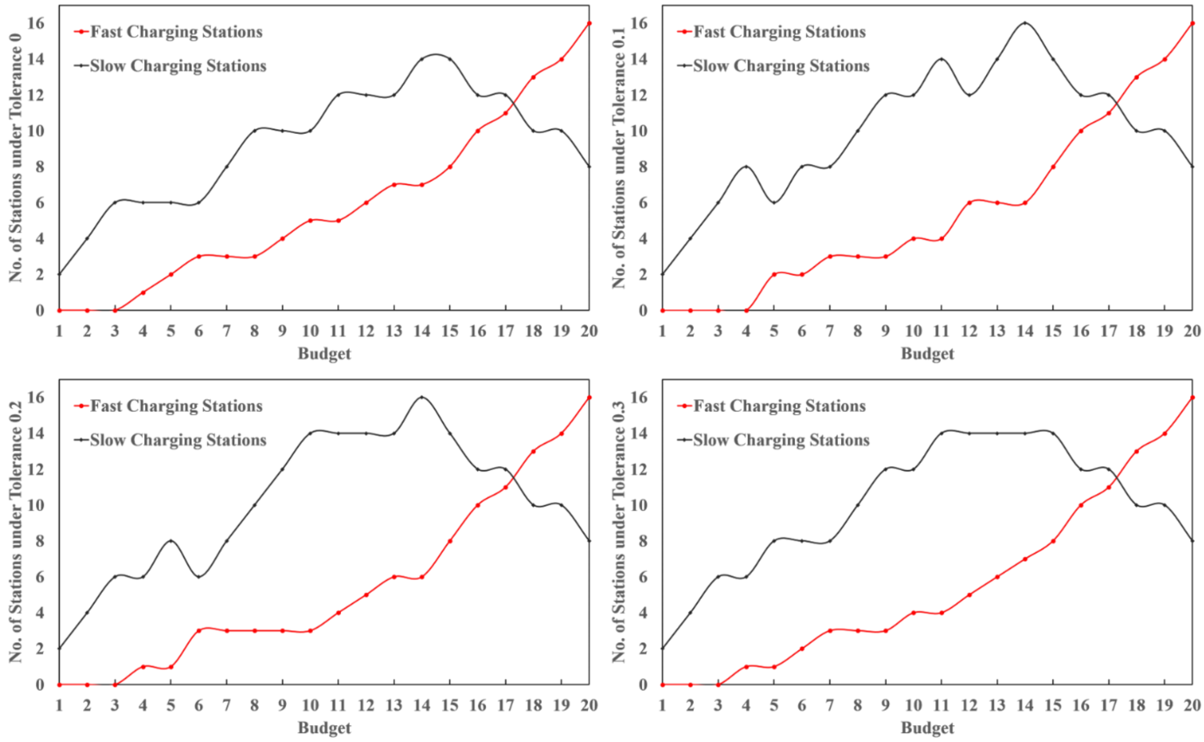

Figure 7 Variations of the number of fast and slow charging stations under different cost deviation tolerances.

4.3.4 Station operation suggestions

To analyze the workload of each charging station, we calculate the number of flows served by each station as budget varies from 1 to 20 under the tolerance of 0, 0.1, 0.2, and 0.3, as shown in Table 7 to Table 10. Clearly, the workload of these stations distinct from each other significantly. For example, when the EV users accept at most a 10% increase in the travel cost and 12 unit costs will be invested in the station construction, the busiest location - location 1 - serves nearly 25,000 flows. By contrast, the least-busy location - location 21 - serves around 2,000 flows, less than 8% of the flows through location 1. The locations that are often chosen by the model to locate charging stations generally have a large number of flows passing through them and are often the origins or destinations of OD pairs with a large flow volume. Besides, the intersection of multiple highways is also easily be chosen by the model. These locations can be regarded as the traffic pivot on the network and should be prosperous cities in Zhejiang. As a matter of fact, location 1 is the capital of Zhejiang Province - Hangzhou - which has over 10 million population, and is connected with eight highway corridors; whereas location 21 is a small city located in the southeast corner of Zhejiang Province, and its population is less than 1 million. This fact coincides with our analysis that the model tends to locate charging stations at locations with high traffic flows. Allowing a larger tolerance for travel cost deviation generally makes the workload of a particular station increase. For instance, given the budget being 12, the traffic flows served by location 2 under tolerance of 0, 0.1, 0.2, and 0.3 are 16,142, 17,219, 19,510, and 19,836, respectively. This could be explained by that as more additional travel costs being acceptable, the EV users could make a detour to far stations for refueling so that the total served flows get increased.

Table 7 Traffic flows served by each station with the increase of budget under the tolerance of 0.

No. Flows / City/Loc No.		B 1	2	3	4	5	6	7	8	9	10	11	12	13	14	15	16	17	18	19	20
Hangzhou	1	0	0	0	0	0	14,368	17,338	19,723	19,723	20,548	22,329	23,297	23,297	23,509	24,230	24,344	25,027	25,219	25,544	25,544
Ningbo	2	0	0	0	0	7,065	10,174	12,313	12,564	14,392	15,175	15,175	16,142	16,142	17,903	18,017	18,175	18,175	18,367	18,367	18,526
Wenzhou	3	0	0	0	0	0	0	0	0	0	0	0	18,286	21,286	21,399	22,362	22,634	22,634	22,868	22,868	22,868
Shaoxing	4	6,992	6,992	7,636	10,041	9,795	10,227	11,808	12,100	12,100	15,039	15,331	15,457	15,457	15,457	15,457	15,457	15,617	15,617	15,617	15,776
Taizhou	5	0	0	0	0	9,174	9,174	9,174	9,174	11,377	14,051	14,051	15,104	15,295	15,655	15,655	15,927	15,927	15,927	15,927	15,927
Jinhua	6	0	0	0	0	0	0	0	0	0	4,574	4,574	7,087	8,509	9,827	11,024	11,024	11,024	11,024	11,024	11,024
Quzhou	7	0	0	0	0	0	0	0	0	0	0	0	0	0	1,549	1,794	1,794	2,477	2,477	2,477	2,477
Huzhou	8	0	0	0	0	0	0	2,520	2,520	2,520	2,672	2,672	2,898	2,898	2,898	3,057	3,057	3,057	3,057	3,382	3,382
Jiaxing	9	0	2,978	0	2,978	4,205	5,035	5,035	5,327	5,981	5,802	5,981	6,352	6,352	6,352	6,352	6,757	6,878	6,878	7,203	7,203
Zhoushan	10	0	0	0	0	0	0	0	0	0	0	0	0	0	1,566	1,566	1,566	1,566	1,566	1,566	1,725
Lishui	11	0	0	0	0	0	0	0	0	0	0	0	2,700	4,356	4,356	5,319	5,319	5,319	5,553	5,553	5,553
Jiande	12	0	0	0	0	0	0	0	0	0	0	0	0	0	0	0	0	683	683	683	683
Cixi	13	0	0	0	2,745	0	7,182	7,670	7,670	8,688	8,688	8,688	8,641	8,641	8,853	8,853	9,419	9,419	9,611	9,611	9,611
Yuyao	14	0	0	2,407	4,812	4,566	0	5,016	5,016	5,267	5,267	5,267	5,156	5,156	5,156	5,156	5,267	5,267	5,267	5,267	5,426
Ruian	15	5,995	6,251	5,995	5,995	6,602	6,602	6,602	6,602	6,745	6,745	6,745	6,745	8,706	8,706	8,582	8,582	8,582	8,706	8,706	8,706
Yueqing	16	0	4,949	0	0	8,838	5,027	8,838	8,838	11,626	12,336	12,336	13,389	13,810	13,923	13,813	14,085	14,085	14,195	14,195	14,195
Cangnan	17	0	0	0	0	0	0	0	0	0	0	0	0	1,707	1,707	1,707	1,707	1,707	1,707	1,707	1,707
Zhuji	18	0	0	0	0	0	0	0	2,570	2,570	0	3,924	5,251	5,251	5,251	6,089	6,203	6,203	6,395	6,395	6,395
Xinchang	19	0	0	0	0	0	0	0	0	0	4,790	4,790	5,088	5,088	5,394	5,508	5,394	5,394	5,394	5,394	5,394
Yuhuan	20	0	0	0	0	0	0	0	0	0	0	0	0	0	0	0	0	0	0	0	0
Wenling	21	0	0	0	0	0	0	0	0	1,849	1,962	1,962	1,962	1,962	1,962	1,962	1,962	1,962	1,962	1,962	1,962
Linhai	22	0	0	2,846	2,846	5,150	5,150	5,150	5,150	6,978	9,914	9,914	10,709	10,709	11,069	11,069	11,341	11,341	11,341	11,341	11,341
Yiwu	23	0	0	0	0	0	0	0	2,458	2,458	5,940	5,940	7,684	7,856	8,162	9,114	9,114	9,114	9,114	9,114	9,114
Dongyang	24	0	0	0	0	0	0	0	0	0	0	0	0	0	0	0	0	0	0	0	0
Lanxi	25	0	0	0	0	0	0	0	0	0	0	0	0	0	0	0	0	0	0	0	0
Yongkang	26	0	0	0	0	0	0	0	0	0	0	0	0	0	0	3,943	3,943	3,943	3,943	3,943	3,943
Jiangshan	27	0	0	0	0	0	0	0	0	0	0	0	0	0	0	0	0	0	0	0	0
Deqing	28	0	0	0	0	0	0	0	0	0	0	0	0	0	0	0	0	0	0	3,382	3,382
Changxing	29	0	0	0	0	0	0	0	0	0	0	0	0	0	0	0	0	0	0	0	0
Anji	30	0	0	0	0	0	0	0	0	0	0	0	0	0	0	0	0	0	0	0	0
Pinghu	31	0	0	0	0	0	0	0	0	0	0	0	0	0	0	0	0	0	0	0	0
Tongxiang	32	0	0	0	0	0	0	0	0	0	0	0	0	0	0	0	0	0	0	0	0
Haining	33	0	0	0	0	0	0	0	0	0	0	0	0	0	0	0	0	0	0	0	0
Longquan	34	0	0	0	0	0	0	0	0	0	0	0	0	0	0	0	0	0	0	0	0

Table 8 Traffic flows served by each station with the increase of budget under the tolerance of 0.1.

City/Loc No. \ No. Flows		B 1	2	3	4	5	6	7	8	9	10	11	12	13	14	15	16	17	18	19	20
Hangzhou	1	0	0	0	0	0	14,935	18,846	21,404	21,502	23,602	23,649	24,596	24,710	25,254	25,439	25,439	25,364	25,389	25,364	25,387
Ningbo	2	0	0	0	0	10,416	10,562	15,769	16,553	16,864	16,578	17,898	17,219	17,135	18,456	18,456	18,480	18,597	18,640	18,621	18,640
Wenzhou	3	0	0	0	0	0	0	0	0	0	0	0	20,872	22,417	22,433	22,786	22,776	22,786	22,797	22,821	22,825
Shaoxing	4	6,992	9,752	9,752	7,973	9,338	11,321	11,938	12,361	12,100	15,959	16,084	16,251	16,379	16,520	15,894	16,570	16,570	15,776	16,405	15,776
Taizhou	5	0	0	0	5,442	11,055	5,243	9,204	12,050	12,927	14,993	15,227	16,454	16,659	16,704	16,062	16,693	16,704	15,927	16,556	15,927
Jinhua	6	0	0	0	0	0	0	0	0	0	4,962	4,962	8,617	10,001	9,873	10,807	10,166	10,166	10,953	10,348	10,981
Quzhou	7	0	0	0	0	0	0	0	0	0	0	0	0	1,878	2,248	2,461	2,461	2,461	2,455	2,477	2,477
Huzhou	8	0	0	0	0	0	0	3,060	3,060	3,060	3,098	3,098	3,330	3,330	3,330	3,330	3,330	3,376	3,376	3,382	3,373
Jiaxing	9	0	0	2,978	3,331	5,197	6,229	6,306	6,729	6,598	6,598	6,598	6,984	6,984	6,984	7,105	7,157	7,203	7,203	7,203	7,203
Zhoushan	10	0	0	0	0	0	0	0	0	0	0	1,684	0	0	1,691	1,691	1,725	1,725	1,725	1,725	1,725
Lishui	11	0	0	0	0	0	0	0	0	0	0	0	4,140	4,341	4,341	5,336	4,695	4,695	5,482	4,877	5,510
Jiande	12	0	0	0	0	0	0	0	0	0	0	0	0	0	498	683	683	683	683	683	683
Cixi	13	0	0	0	2,852	5,138	5,632	10,235	10,408	10,506	9,438	9,485	9,483	9,483	9,530	9,530	9,581	9,575	9,611	9,592	9,611
Yuyao	14	0	4,523	4,523	2,744	0	5,131	5,384	5,514	5,254	5,254	5,378	5,260	5,260	5,385	5,385	5,410	5,419	5,426	5,426	5,426
Ruian	15	5,995	6,251	6,251	5,995	6,745	5,995	6,745	6,745	8,452	6,745	8,452	6,938	8,645	8,645	8,706	8,706	8,706	8,706	8,706	8,706
Yueqing	16	0	4,949	4,949	2,596	9,968	2,845	10,214	10,214	12,352	13,170	13,376	14,712	14,903	14,919	14,330	14,961	14,972	14,195	14,824	14,195
Cangnan	17	0	0	0	0	0	0	0	0	1,707	0	1,707	0	1,707	1,707	1,707	1,707	1,707	1,707	1,707	1,707
Zhuji	18	0	0	0	0	0	0	0	3,039	3,039	4,393	4,393	5,408	5,522	5,522	6,176	5,534	5,414	6,233	5,586	6,238
Xinchang	19	0	0	0	0	0	0	0	0	0	5,511	5,511	6,259	6,316	6,188	5,547	6,188	6,302	5,508	6,137	5,508
Yuhuan	20	0	0	0	0	0	0	0	0	0	0	0	0	0	0	0	0	0	0	0	0
Wenling	21	0	0	0	0	0	0	0	0	1,947	1,962	1,962	1,962	1,962	1,962	1,962	1,962	1,962	1,962	1,962	1,962
Linhai	22	0	0	2,846	2,846	7,586	2,763	5,491	8,696	9,007	11,410	11,454	12,059	12,073	12,118	11,476	12,107	12,118	11,341	11,970	11,341
Yiwu	23	0	0	0	0	0	0	0	2,754	2,754	6,328	6,328	8,181	8,353	8,225	8,913	8,272	8,272	9,066	8,438	9,071
Dongyang	24	0	0	0	0	0	0	0	0	0	0	0	0	0	0	0	0	0	0	0	0
Lanxi	25	0	0	0	0	0	0	0	0	0	0	0	0	0	0	0	0	0	0	0	1,794
Yongkang	26	0	0	0	0	0	0	0	0	0	0	0	0	0	0	0	0	0	0	3,267	3,900
Jiangshan	27	0	0	0	0	0	0	0	0	0	0	0	0	0	0	0	0	0	0	0	0
Deqing	28	0	0	0	0	0	0	0	0	0	0	0	0	0	0	0	0	3,376	3,376	3,382	3,373
Changxing	29	0	0	0	0	0	0	0	0	0	0	0	0	0	0	0	0	0	0	0	0
Anji	30	0	0	0	0	0	0	0	0	0	0	0	0	0	0	0	0	0	0	0	0
Pinghu	31	0	0	0	0	0	0	0	0	0	0	0	0	0	0	0	0	0	0	0	0
Tongxiang	32	0	0	0	0	0	0	0	0	0	0	0	0	0	0	0	0	0	0	0	0
Haining	33	0	0	0	0	0	0	0	0	0	0	0	0	0	0	0	0	0	0	0	0
Longquan	34	0	0	0	0	0	0	0	0	0	0	0	0	0	0	0	0	0	0	0	0

Table 9 Traffic flows served by each station with the increase of budget under the tolerance of 0.2.

No. Flows / City/Loc No.		B																			
		1	2	3	4	5	6	7	8	9	10	11	12	13	14	15	16	17	18	19	20
Hangzhou	1	0	0	0	0	0	0	20,352	22,543	24,054	23,707	24,908	25,017	24,716	25,214	25,323	25,324	25,125	25,503	25,493	25,473
Ningbo	2	0	0	0	0	0	15,129	15,162	17,596	17,635	18,198	17,311	19,510	18,540	18,570	18,570	18,604	18,849	18,526	18,526	18,504
Wenzhou	3	0	0	0	0	0	0	0	0	0	0	21,740	22,504	22,401	22,433	22,784	22,785	22,784	22,804	22,825	22,819
Shaoxing	4	6,992	9,752	10,396	9,416	10,734	14,460	11,399	12,880	12,989	12,730	13,044	13,164	16,481	16,520	16,534	15,928	15,776	16,570	16,559	16,411
Taizhou	5	0	0	0	0	0	13,027	13,385	13,492	13,570	13,079	13,389	14,693	16,690	16,704	16,701	16,061	15,908	16,721	16,719	16,562
Jinhua	6	0	0	0	0	0	0	0	4,285	4,580	4,580	8,831	8,849	8,965	9,947	10,166	10,807	10,959	10,166	10,172	10,339
Quzhou	7	0	0	0	0	0	0	0	0	0	0	0	0	0	2,322	2,461	2,461	2,461	2,461	2,477	2,477
Huzhou	8	0	0	0	0	0	0	3,181	3,181	3,181	3,181	3,273	3,297	3,330	3,330	3,328	3,329	3,376	3,376	3,373	3,373
Jiaxing	9	0	0	4,558	4,733	4,836	5,927	6,694	6,694	6,747	6,747	6,912	7,058	7,058	7,058	7,105	7,157	7,203	7,203	7,203	7,203
Zhoushan	10	0	0	0	0	0	0	0	0	0	1,632	0	1,691	1,691	1,691	1,691	1,725	1,725	1,725	1,725	1,725
Lishui	11	0	0	0	0	0	0	0	0	0	0	5,240	5,281	4,309	4,341	4,695	5,336	5,488	4,695	4,709	4,868
Jiande	12	0	0	0	0	0	0	0	0	0	0	0	0	0	498	683	683	683	683	683	683
Cixi	13	0	0	3,717	4,002	4,114	5,126	10,583	10,695	10,734	10,387	10,195	10,560	9,530	9,530	9,530	9,582	9,581	9,611	9,603	9,589
Yuyao	14	0	4,523	4,664	2,173	4,817	8,582	0	5,580	5,580	5,322	5,528	5,723	5,385	5,385	5,385	5,419	5,665	5,426	5,426	5,426
Ruian	15	5,995	6,477	6,477	6,346	6,715	6,827	6,827	6,827	8,421	8,421	8,463	8,645	8,645	8,645	8,706	8,706	8,706	8,706	8,706	8,706
Yueqing	16	0	5,175	5,175	2,995	8,301	11,359	11,893	11,906	11,984	12,735	13,242	14,266	14,919	14,919	14,969	14,329	14,176	14,989	14,987	14,830
Cangnan	17	0	0	0	0	0	0	0	0	1,707	1,707	1,668	1,707	1,707	1,707	1,707	1,707	1,707	1,707	1,707	1,707
Zhuji	18	0	0	0	0	2,451	0	0	0	5,259	5,259	6,799	6,799	5,482	5,482	5,420	6,062	6,214	5,553	5,552	5,689
Xinchang	19	0	0	0	0	0	0	0	0	0	0	0	0	6,364	6,302	6,300	5,660	5,508	6,188	6,177	6,029
Yuhuan	20	0	0	0	0	0	0	0	0	0	0	0	0	0	0	0	0	0	0	0	0
Wenling	21	0	0	0	0	0	0	0	0	0	1,897	1,740	1,947	1,962	1,962	1,962	1,962	1,962	1,962	1,962	1,962
Linhai	22	0	0	0	862	3,784	8,737	9,119	9,226	9,226	8,604	8,632	9,646	12,104	12,118	12,115	11,475	11,322	12,135	12,133	11,976
Yiwu	23	0	0	0	0	2,357	0	3,056	5,444	5,739	5,739	7,723	7,723	8,360	8,299	8,272	8,913	9,066	8,272	8,262	8,429
Dongyang	24	0	0	0	0	0	0	0	0	0	0	0	0	0	0	0	0	0	0	0	0
Lanxi	25	0	0	0	0	0	0	0	0	0	0	0	0	0	0	0	0	0	0	0	0
Yongkang	26	0	0	0	0	0	0	0	0	0	0	0	0	0	0	0	0	0	0	3,099	3,258
Jiangshan	27	0	0	0	0	0	0	0	0	0	0	0	0	0	0	0	0	0	0	0	0
Deqing	28	0	0	0	0	0	0	0	0	0	0	0	0	0	0	0	0	3,376	3,376	3,373	3,373
Changxing	29	0	0	0	0	0	0	0	0	0	0	0	0	0	0	0	0	0	0	0	0
Anji	30	0	0	0	0	0	0	0	0	0	0	0	0	0	0	0	0	0	0	0	0
Pinghu	31	0	0	0	0	0	0	0	0	0	0	0	0	0	0	0	0	0	0	0	0
Tongxiang	32	0	0	0	0	0	0	0	0	0	0	0	0	0	0	0	0	0	0	0	0
Haining	33	0	0	0	0	0	0	0	0	0	0	0	0	0	0	0	0	0	0	0	0
Longquan	34	0	0	0	0	0	0	0	0	0	0	0	0	0	0	0	0	0	0	0	0

Table 10 Traffic flows served by each station with the increase of budget under the tolerance of 0.3.

No. Flows / City/Loc No.		B 1	2	3	4	5	6	7	8	9	10	11	12	13	14	15	16	17	18	19	20
Hangzhou	1	0	0	0	0	0	14,228	20,527	22,543	24,281	25,114	25,137	25,247	24,984	24,913	25,439	25,439	25,371	25,480	25,276	25,298
Ningbo	2	0	0	0	0	0	15,284	15,605	17,922	18,059	17,417	17,637	19,836	18,426	18,570	18,456	18,490	18,604	18,507	18,750	18,772
Wenzhou	3	0	0	0	0	0	0	0	0	0	20,029	21,740	22,504	22,401	22,786	22,786	22,786	22,786	22,868	22,868	22,868
Shaoxing	4	6,992	9,752	10,396	10,586	10,924	11,531	11,900	13,206	13,378	13,445	13,445	13,565	16,481	16,351	15,894	15,929	15,929	15,776	15,776	15,776
Taizhou	5	0	0	0	0	0	13,320	13,732	13,766	14,347	13,145	13,664	14,968	16,690	16,551	16,062	16,062	16,062	15,927	15,927	15,927
Jinhua	6	0	0	0	0	0	0	0	4,285	5,737	9,504	9,455	9,474	9,514	10,718	10,807	10,807	10,960	11,024	11,024	11,024
Quzhou	7	0	0	0	0	0	0	0	0	0	0	0	0	0	2,177	2,461	2,461	2,461	2,477	2,477	2,477
Huzhou	8	0	0	0	0	0	0	3,181	3,181	3,181	3,273	3,273	3,297	3,330	3,330	3,330	3,330	3,376	3,336	3,382	3,382
Jiaxing	9	0	0	4,558	4,864	5,169	5,600	6,694	6,694	6,747	6,912	6,912	7,058	7,058	7,058	7,105	7,157	7,203	7,157	7,203	7,203
Zhoushan	10	0	0	0	0	0	0	0	0	0	0	0	1,691	1,691	1,691	1,691	1,725	1,725	1,725	1,725	1,725
Lishui	11	0	0	0	0	0	0	0	0	1,659	5,289	5,240	5,281	4,309	4,847	5,336	5,336	5,489	5,553	5,553	5,553
Jiande	12	0	0	0	0	0	0	0	0	0	0	0	0	0	0	683	683	683	683	683	683
Cixi	13	0	0	3,717	4,245	4,381	8,486	10,628	10,695	10,734	10,122	10,195	10,560	9,530	9,530	9,530	9,582	9,582	9,592	9,589	9,611
Yuyao	14	0	4,523	4,664	5,007	5,007	5,980	0	5,906	5,906	5,854	5,854	6,049	5,385	5,385	5,385	5,419	5,419	5,426	5,672	5,672
Ruian	15	5,995	6,477	6,477	6,715	6,715	6,827	6,827	6,827	6,963	6,908	8,463	8,645	8,645	8,706	8,706	8,706	8,706	8,706	8,706	8,706
Yueqing	16	0	5,175	482	8,872	8,872	12,075	12,275	12,288	12,987	11,893	13,242	14,266	14,919	14,819	14,330	14,330	14,330	14,195	14,195	14,195
Cangnan	17	0	0	0	0	0	0	0	0	0	0	1,668	1,707	1,707	1,707	1,707	1,707	1,707	1,707	1,707	1,707
Zhuji	18	0	0	0	0	2,789	0	0	0	5,487	7,077	7,028	7,028	5,750	5,844	6,176	6,176	6,214	6,376	6,373	6,395
Xinchang	19	0	0	0	0	0	0	0	0	0	0	0	0	6,250	6,277	5,547	5,547	5,661	5,394	5,394	5,394
Yuhuan	20	0	0	0	0	0	0	0	0	0	0	0	0	0	0	0	0	0	0	0	0
Wenling	21	0	0	0	0	0	0	0	0	0	0	1,740	1,947	1,962	1,962	1,962	1,962	1,962	1,962	1,962	1,962
Linhai	22	0	0	0	4,104	4,104	9,078	9,517	9,552	9,650	8,738	8,958	9,972	12,104	11,965	11,476	11,476	11,476	11,341	11,341	11,341
Yiwu	23	0	0	0	0	2,606	0	3,056	5,444	5,967	8,002	7,953	7,953	8,515	8,824	8,913	8,913	9,066	9,114	9,114	9,114
Dongyang	24	0	0	0	0	0	0	0	0	0	0	0	0	0	0	0	0	0	0	0	0
Lanxi	25	0	0	0	0	0	0	0	0	0	0	0	0	0	0	0	0	0	0	0	0
Yongkang	26	0	0	0	0	0	0	0	0	0	0	0	0	0	0	0	0	0	3,943	3,943	3,943
Jiangshan	27	0	0	0	0	0	0	0	0	0	0	0	0	0	0	0	0	0	0	0	0
Deqing	28	0	0	0	0	0	0	0	0	0	0	0	0	0	0	0	0	3,376	0	3,382	3,382
Changxing	29	0	0	0	0	0	0	0	0	0	0	0	0	0	0	0	0	0	0	0	0
Anji	30	0	0	0	0	0	0	0	0	0	0	0	0	0	0	0	0	0	0	0	0
Pinghu	31	0	0	0	0	0	0	0	0	0	0	0	0	0	0	0	0	0	0	0	0
Tongxiang	32	0	0	0	0	0	0	0	0	0	0	0	0	0	0	0	0	0	0	0	0
Haining	33	0	0	0	0	0	0	0	0	0	0	0	0	0	0	0	0	0	0	0	0
Longquan	34	0	0	0	0	0	0	0	0	0	0	0	0	0	0	0	0	0	0	0	0

Based on the above analysis, we understand that both budget and tolerance for cost deviation largely affect the workload of a certain station. Thus, when operating a charging station system, the operators are expected to equip more charging piles and workers at the busy stations while installing fewer chargers and workers at the idle stations. Meanwhile, since some busy stations could serve lots of EVs simultaneously, the government must enhance the power grid around these locations for electricity safety. Furthermore, these busy stations could be congested due to excessive charging demands, which also requires the operator to improve the service quality of these stations. The government may organize activities at these busy stations with high public exposure to advertising green transportation and other related policy, e.g., EV purchase incentives. To improve the utility of idle stations and at the same time, to divert the workload of busy stations, the government may impose a charging subsidy policy among these stations. In particular, the charging price at idle stations should be reduced while the charging price at busy stations can be increased, especially during peak charging hours. The developing countries of BRI are strongly recommended to adopt such a subsidy policy since it can alleviate the workload of busy stations and to improve idle stations' utility, making governments' station operation policy more economical and efficient. Furthermore, balancing charging demand can mitigate the pressure on the power grid and avoid the formation of hidden safety hazards, which is particularly important for some countries and regions with underdeveloped power technology.

4.3.5 Deploying charging stations in multiple stages

As the government aims to promote green transportation, the public's environmentally friendly awareness and acceptance of traveling by EVs are expected to advance. Reflected in the modeling perspective, it is the increase of travelers' tolerance for travel cost deviation. The change of tolerance may significantly influences the station deployment. To see that, we deploy stations with 12 unit budgets under tolerances 0 and 0.3, respectively. Under tolerance 0, the fast charging stations should be built at locations 1, 2, 3, 5, 6, 19 and the slow charging stations should be at locations 4, 8, 9, 11, 13, 14, 15, 16, 18, 21, 22, 23. Under tolerance 0.3, the optimal locations for fast and slow charging stations are 1, 2, 3, 5, 6 and 4, 8, 9, 10, 11, 13, 14, 15, 16, 17, 18, 21, 22, 23, respectively. When EV users accept a higher cost deviation, there is no need to assign a fast charging station at location 19. Instead, the saved cost can be used to build two slow charging stations at locations 10 and 17. Accordingly, the covered flow volume rises from 63,393 to 69,487 as tolerance changes from 0 to 0.3. In the real world, it may be impractical for the government to remove station 19, although station 19 becomes redundant when travelers' tolerance increases to 0.3. A way to cope with this problem is to implement infrastructure projects in several stages. This enables the government to modify the project according to travelers' changing behaviors, specifically the tolerance in this study. Ideally, the charging stations installed in the future stages should complement these in early stages, so as to cover as many flows as possible after the travelers' tolerance increases.

Now we consider a mid-term plan, i.e., two stages, to further illustrate the above idea. Suppose the government will invest 7 unit budget at each stage and travelers' tolerance rises from 0 to 0.3. To satisfy the charging demand at stage 1, we use the proposed approach to maximize the flow coverage under tolerance 0 and budge 7. As shown in Table 11, the resultant station deployment is locations 1, 2, 5 for fast charging stations and locations 4, 8, 9, 13, 14, 15, 16, 22 for slow charging stations. As for stage 2, we maximize the flow coverage under tolerance 0.3 and budget 14. The result suggests fast charging station to be built at locations 1, 2, 3, 5, 6, 11, 19 and slow charging stations at locations 4, 7, 8, 9, 10, 13, 14, 15, 16, 17, 18, 21, 22, 23. By comparing the two deployment plans, at stage 2, we should build fast charging stations at locations 6, 11, 19 and slow charging stations at locations 17, 18, 21, 23.

To conclude, the government should first estimate travelers' tolerance for travel cost deviation at stages 1 and 2, which can be done by survey. Then, under the given total budget, the government needs to assign the investment at stages 1 and 2. For stage 1, we use the proposed approach to maximize flow coverage under the tolerance and the budget for stage 1 and obtain the deployment plan for stage 1. As for stage 2, we maximize flow coverage under the tolerance of stage 2 and the total budget of all stages. Then, we compare the obtained deployment with the plan of stage 1 to find which stations should be added. These added stations are the deployment plan for stage 2. Note that the problem solved at each stage is static. Briefly, at a certain stage, we maximize the flow coverage with the tolerance of and the budget allocated to this stage. The obtained deployment excluding the stations previously built is the deployment plan of this stage. The inputs of each stage are assumed to be estimated or given by the operator. Analytically modeling the uncertainty of parameters in future stages requires other sophisticated techniques, e.g., stochastic or robust optimization, which goes beyond the focus of this study.

Table 11 Comparison of two stages in a mid-term station deployment plan.

	Stage I	Stage II
Tolerance	0.1	0.3
Budget	7	14
No. Flows	53609	72640
Fast Station No.	1, 2, 5	1, 2, ***3***, 5, ***6***, ***11***, ***19***
Slow Station No.	4, 8, 9, 13, 14, 15, 16, 22	4, ***7***, 8, 9, ***10***, 13, 14, 15, 16, ***17***, ***18***, ***21***, 22, ***23***

4.4 Policy outlook

Following the fast advancement of battery technology, it is foreseeable that the EVs will be increasingly adaptable to long-distance trips in the future. However, larger battery capacity will bring about an increase in charging time, and accordingly, a more efficient charging service would be desirable for the EV users. Thus, widely building fast charging stations more aligns with the development trend of travelers' improving requirements. On the other hand, with the quickly evolving charging technology, even the currently state-of-art charging facilities are possible to become out-of-date in the next few years. The charging facility replacement and renovation will inevitably call for a large amount of investment. Hence, to reduce the renovation costs, the government is expected to adopt more replaceable equipment when constructing charging stations, such as modular equipment, which can be partly replaced in the renovation. Also, the government is supposed to improve the power grid load to ensure electricity safety as well as to support potential peak power consumption.

As the EVs are gaining more and more popularity, the charging demand for EVs will definitely get increased. The charging stations will be more closely connected with EV users' life and travel and are likely to be the pivot joining people's lives and the future Internet of Things (IoT). The data contained in the charging station has great value, such as EV users' behavioral data (e.g., travel trajectory and station choices), battery charging data (e.g., charging and discharging process), as well as power grid data (e.g., potential safety hazard and peak valley values). These data will help us better understand EV users' preferences and habits for improving service quality and regulate the construction of charging stations and ensure the safety level. In addition to assisting in IoT connection and policy-making, the data can also be used in research areas such as emerging battery and charging technologies.

Promoting charging station construction on a large scale not only requires financial support but also needs land policy support so that we can allocate these stations in a reasonable deployment. In this process, the central government plays a crucial role in responsible for the top-level design, i.e., entailing favorable financial and land policies for charging station construction together with green transportation advertisements. For instance, allocate dedicated funds for the construction of charging stations; sell the land for charging stations at low prices; subsidize the purchase of electric vehicles; and subsidize the charging fees. When the local governments optimize the station deployment in their administration areas, they should combine the regional charging demands and policies for better adapting to local conditions. In particular, for the developed countries in the BRI, the government could locate more fast charging stations domestically to provide efficient charging services and adapt to future increasing charging demands. In contrast, in the developing countries in the BRI and other nations with a limited budget, they are expected to prioritize slow charging station construction so that more travel routes can be covered. Furthermore, the government could also build fast charging stations at metropolitans, especially in the cities with a high EV penetration rate, while locating slow charging stations in villages and rural areas. These two types of stations can be geographically complementary to each other.

The increase of charging stations could put more challenges to the power facilities. Companying with the promotion of charging facility construction, the power grids should be also upgraded at the same time to be adaptable to high-power charging loads. Meanwhile, the government is expected to actively conduct advertisement and education of green transportation in the public. For example, the EV users are encouraged to refuel their vehicles in low power consumption valleys and accept staggered charging. Furthermore, the supporting policy towards unifying the standard of station construction and operation is anticipated to facilitate coordination and communication in a holistic management perspective. Finally, the collaboration between the local governments and enterprises, which is popular in many commercial activities, can be referenced to share the costs of construction and operation. It may be a good choice to allocate the stations nearby large shopping malls and ask the shopping malls to afford part of the costs, e.g., buying lands and hiring workers. The charging stations will attract more travelers for the malls, beneficial for both the government and the enterprise.

5. Conclusions and future research

This study investigates the optimal deployment of charging stations, i.e., fast and slow charging stations, for flow coverage maximization under the limited budget while taking EV users' partial charging behavior and elastic demand. The travelers are assumed to accept a cost deviation travel path aside from the minimum cost travel path and the additional cost will result in travel demand decline. To solve this problem, we propose a two-phase approach that first quickly finds high-quality station deployment and then utilizes the obtained deployment plan to expedite the model solving of the considered location problem. To efficiently find high-quality station deployment plans, we develop a two-layer heuristic based on the simulated annealing framework. A deployment generation rule based on the flows passing through each candidate location is devised to construct promising deployment plans in the outer layer. The flow coverage of the generated deployment is assessed in the inner layer to refine the deployment generation rule. Leveraging the convexity of the elastic demand function and the inverse relationship of GTC and covered flows, we propose a mixed-integer linear programming model that can quickly find the flow coverage, which further enhances the algorithm efficiency. The performance of the proposed two-phase approach is examined on the highway network of Zhejiang, China by numerical experiments. The results show that our approach significantly outperforms the existing algorithm for the DMCS problem in the computation time, particularly under a difficult parameter setting such as permitting a high travel cost deviation tolerance.

Considering travelers' behavioral characteristics in charging station location optimization provides policymakers with some insightful implications from five perspectives. Notably, we found that (a) Given a higher cost deviation being accepted by travelers, the predesignated budget can satisfy more charging demands. In other words, by encouraging travelers to accept a reasonable additional travel cost through advertising green transportation and transport electrification, governments could serve more EV users under a limited budget or use less investment to accomplish the target demand fulfillment, resulting in a more economical policy. (b) As the available investment rises, the growth rate of flow coverage slows down gradually, especially after the ratio of covered flow volume reaches 95%. As a matter of fact, a high flow coverage ratio can be achieved with very limited funds. Thus, we strongly recommend that governments set a reasonable target of charging demand fulfillment, such as 85%-95%, rather than substantially invest to satisfy all demands, so as to ensure the efficient utilization of the investment. (c) Densely populated cities and the intersection of multiple highways are more favorable to be chosen as a charging station location, especially locating fast charging stations; on the contrary, small cities are much less likely to be assigned a charging station. Therefore, we recommend governments to policy practice in large cities and transportation hubs, with emphasis on budget and policy support. (d) It is observed that the workload between charging stations differs from each other significantly. The busiest station serves more than ten times as many users as the least-busy station, suggesting a charging demand imbalance among stations. Operators could equip these busy stations with more charging piles and workers, as well as upgrade the supporting power grid to ensure electricity during peak demand times. Also, pricing strategies, which is widely used in transportation management (Eliasson, 2021), may be incorporated to alleviate the imbalanced workload among stations. For example, applying different charging prices between busy and idle stations to mitigate the work pressure of busy stations and increase the efficiency of idle stations. (e) It can be foreseeable that after regulators advertise for green transportation, the popularity of EVs and travelers' cost deviation tolerance would get increased over time. Therefore, governments should take into account travelers' changing tolerance when devising a mid- or long-term station construction plan. In particular, the pre-positioned charging stations and the post-positioned stations are expected to together form the optimal deployment after travelers' cost deviation tolerance gets increased.

Further research can be conducted in several directions. First, due to the limited capacity of charging stations in the real world, users may have to wait for being served. The queueing behavior at the charging station can be modeled in the future. Second, the travel time of each link is assumed to be known in advance in this paper while in practice the travel time may increase due to the traffic congestion. The impact of traffic congestion can be incorporated into the location model to depict EV users' travel costs more precisely. Third, instead of the linear charging profile adopted in this study, we can consider other realistic charging profiles and the impact of EV's own properties, e.g., the battery thermal effect (Liao et al., 2021), on battery charging and discharging in locating charging stations, which enables the model to be more powerful and the location strategy to be more realistic.

Acknowledgments

This research is supported by the National Natural Science Foundation of China (No. 71901189), the Research Grants Council of the Hong Kong Special Administrative Region, China (PolyU 25207319), and the Hong Kong Polytechnic University (1-BE1V).

Appendixes

Appendix 1. Notations

N	Set of locations
A	Set of links
S	Set of candidate locations for building charging stations
W	Set of OD pairs
i, j	Indices for locations
s	Index for candidate locations
$o(w)$	Origin of OD pair w
$d(w)$	Destination of OD pair w
w	Index for OD pairs
q	Index for station types
B	Total budget
E	Battery capacity measured in kWh
b_s^q	Cost of building type q station at location s
E_O	Initial SOC at origins
E_D	Minimum SOC after arriving at destinations
t_{ij}	Travel time along link (i, j)
e_{ij}	Electricity consumption of link (i, j)
α_q	Fixed time of charging at type q stations
β_q	Fixed cost of charging at type q stations
φ_q	Time consumption per kWh of charging at type q stations
λ_q	Cost per kWh of charging at type q stations
υ	Travelers' value-of-time measured in \$/h
C^w	Minimum GTC of OD pair w
δ^w	Tolerance for cost deviation of OD pair w
θ^w	Sensitivity to cost deviation of OD pair w
F^w	Flows between OD pair w under cost C^w
$f^w(\bullet)$	Convex elastic demand function with respect to GTC
x_{ij}^w	Binary variable which equals 1 if the path flow between OD pair w traverses link (i, j) and 0 otherwise
z^w	Binary variable which equals 1 if OD pair w is covered and 0 otherwise
r_s^w	Binary variable which equals 1 if the path flow between OD pair w charges at location s and 0 otherwise
p_s^w	Continuous variable representing the charging amount at location s for OD pair w
e_i^w	Continuous variable denoting the remaining SOC upon exiting location i for OD pair w
c^w	Continuous variable expressing the generalized travel cost of OD pair w
y_s^{slow}	Value of the slow charging station location variable in the LP relaxation of the model [OP-II]
y_s^{fast}	Value of the slow charging station location variable in the LP relaxation of the model [OP-II]
ϖ_s	Cost ratio of building a fast and a slow charging station at location s

f_s	Flows passing through location s in the LP relaxation of the model [OP-II]
$\tilde{f}_s$	Potential of location s in the deployment initialization process
$\mathcal{S}$	Candidate location sequence in the decreasing order of $\tilde{f}_s$
T	Annealing temperature
l	Iteration number
ε	Annealing ratio
X_{Tabu}	Tabu list for storing low-quality station deployments
$\bar{v}_s$	Flows passing through location s under the current deployment $\bar{D}$
v_s'	Flows passing through location s under the new deployment D'
k	The number of bad locations according to $\bar{v}_s, \forall s \in S$
$\bar{D}$	Current station deployment
$\bar{f}$	Current flow coverage
D^*	Best station deployment
f^*	Best flow coverage
D'	New station deployment
f'	New flow coverage
$\tilde{s}$	Location to be removed for construct new deployments
α_s	Fixed time of charging at location s under a given deployment
β_s	Fixed cost of charging at location s under a given deployment
φ_s	Time per kWh of charging at location s under a given deployment
λ_s	Cost per kWh of charging at location s under a given deployment

Appendix 2. The optimization model for determining the MCTP of OD pair w

[OP-I]

$$\min_{\mathbf{x}, \mathbf{z}, \mathbf{r}, \mathbf{p}, \mathbf{e}} \quad c^w + M\left(1 - z^w\right) \tag{3}$$

subject to

$$c^w = \sum_{i,j \in N:(i,j)\in A} \upsilon t_{ij} x_{ij}^w + \sum_{s\in S} \left(\upsilon a_s + \beta_s\right) r_s^w + \left(\upsilon \varphi_s + \lambda_s\right) p_s^w \tag{4}$$

$$c^w \le \left(1 + \delta^w\right) C^w \tag{5}$$

$$\sum_{j\in N:(i,j)\in A} x_{ij}^w - \sum_{j\in N:(j,i)\in A} x_{ji}^w = \begin{cases} -z^w, & i = o(w) \\ 0 \quad , & i \in N \setminus \left\{o(w), d(w)\right\} \\ z^w \quad , & i = d(w) \end{cases} \tag{6}$$

$$e_{o(w)}^w = \begin{cases} E_O \quad , & o(w) \notin S \\ E_O z^w + p_{o(w)}^w, & o(w) \in S \end{cases} \tag{7}$$

$$e_{d(w)}^w \ge E_D z^w \tag{8}$$

$$\sum_{j\in N:(i,j)\in A} e_{ij} x_{ij}^v \le e_i^v \le E, \quad \forall i \in N \tag{9}$$

$$0 \le p_s^w \le E\gamma_s^w, \quad \forall s \in S \tag{10}$$

$$e_s^w - p_s^w - e_i^w + e_{is} \begin{cases} \le M\left(1 - x_{is}^v\right) \\ \ge M\left(x_{is}^v - 1\right) \end{cases} \quad \forall s \in S, i \in N : (i,s) \in A \tag{11}$$

$$e_j^w - e_i^w + e_{ij} \begin{cases} \le M\left(1 - x_{ij}^v\right) \\ \ge M\left(x_{ij}^v - 1\right) \end{cases} \quad \forall j \in N \setminus S, i \in N : (i,j) \in A \tag{12}$$

$$x_{ij}^w, z_w^v, \gamma_s^v \in \{0,1\}, \quad \forall v \in V, w \in W, s \in S, i,j \in N : (i,j) \in A \tag{13}$$

$$e_i^w, p_s^w \in \mathbb{R}_+, \quad \forall i \in N, s \in S \tag{14}$$

where M is a sufficiently large positive number and $\mathbb{R}_+$ is the set of non-negative real numbers.

The objective function shown by Eq. (3) can be regarded as GTC to complete the trip between OD pair w under the given station deployment plan. If this OD pair is covered, we have $z^w = 1$ and the objective function reduces to c^w. In this case, the proposed model minimizes GTC and we can obtain the model [OP-I] of OD pair w under the given station deployment. If OD pair w cannot be covered, we have $z^w = 0$ and the objective value will be a very large positive number. Since we aim to minimize the objective function, the variable z^w will be forced to be zero if this OD pair can be covered.

Eq. (4) defines GTC of OD pair w, where the first part of its right-hand-side (RHS) is the cost resulted from travel time along highways and the second part represents the cost of charging activities. Constraint (5) suggests that the GTC cannot exceed the pre-specified acceptable threshold. Constraint (6) ensures the flow conservation of the path flow between OD pair w.

Constraints (7)-(12) are the battery charging constraints. In particular, Constraint (7) expresses the initial SOC before departing from the origin. If a charging station locates at the origin of OD pair w, the SOC could be replenished by an amount $p_{o(w)}^w$; otherwise, the SOC upon exiting the origin is E_O. Constraint (8) restricts that the SOC at the destination is above E_D. Constraint (9) indicates the upper and lower bounds of the SOC upon leaving a certain location. The SOC cannot exceed the battery capacity while it should be sufficient to traverse the next link. Constraint (10) limits the maximum refueling amount when charging the battery. Constraints (11) and (12) establish the relationship of the SOC between any two adjacent locations. Specifically, for a candidate location s, if link (i,s) is traversed by the path flow of OD pair w, Constraint (11) reduces to an equality constraint, i.e., $e_s^w - p_s^w = e_i^w - e_{is}$ .The LHS and RHS represent the SOCs upon arriving at location s and exiting location i, respectively, and these two values of SOC should be the same. If the path flow does not traverse link (i,s), Constraint (11) becomes redundant. Likewise, Constraint (12) expresses the SOC relationship of a noncandidate location and its adjacent locations. The variable domains are specified by Constraints (13) and (14).

The proposed model is a mixed-integer linear programming model. In particular, the objective function and all constraints are linear while decision variables contain both integer and continuous variables. The number of constraints is positively proportional to network size and candidate locate set, in particular, $\mathcal{O}\left(|S| \cdot |N|^2\right)$. Hence, for each OD pair, its MCTP has a moderate size and variables and thus generally, can be solved efficiently by off-the-shelf solvers.

Appendix 3. The model [OP-II]

Except for the decision variables x_{ij}^{w}, z^{w}, γ_{s}^{w}, e_{i}^{w}, p_{s}^{w} as defined in the model [OP-I], the model [OP-II] introduces a station location variable $y_{s}^{q} \in \{0,1\}$ for each candidate location $s \in S$ and each station type $q \in Q$, to determine whether type q station is built at location s. A mixed-integer nonlinear programming model was first developed to formulate the DMCS problem. The nonlinear objective function and the nonlinear terms in constraints were then addressed by piece-wise linear approximation and linearization, respectively. The resultant mixed-integer linear programming model is as follows:

[OP-II]

$$\underset{\mathbf{x},\,\mathbf{y},\,\mathbf{z},\,\mathbf{r},\,\mathbf{e},\,\mathbf{p}}{\text{Max}} \quad \sum_{w\in W}\sum_{n=1}^{V(w)} \pi_{n}^{w} f^{w}\left(c_{n}^{w}\right) \tag{15}$$

subject to Eqs. (5)-(12), $\forall w \in W$ and

$$\sum_{s\in S}\sum_{q\in Q} b_{s}^{q} y_{s}^{q} \le B \tag{16}$$

$$\sum_{q\in Q} y_{s}^{q} \le 1, \quad \forall s \in S \tag{17}$$

$$c^{w} = \sum_{i,j\in N:(i,j)\in A} \upsilon t_{ij} x_{ij}^{w} + \sum_{s\in S}\sum_{q\in Q} c1_{s}^{w,q} + c2_{s}^{w,q}, \quad \forall w \in W \tag{18}$$

$$\begin{cases} 0 \le c1_{s}^{w,q} \le \left(\upsilon\varphi_{s}^{q} + \lambda_{s}^{q}\right) E y_{s}^{q} \\ \left(\upsilon\varphi_{s}^{q} + \lambda_{s}^{q}\right)\left[p_{s}^{w} + E\left(y_{s}^{q} - 1\right)\right] \le c1_{s}^{w,q} \le \left(\upsilon\varphi_{s}^{q} + \lambda_{s}^{q}\right) p_{s}^{w} \\ 0 \le c2_{s}^{w,q} \le \left(\upsilon\alpha_{s}^{q} + \beta_{s}^{q}\right) y_{s}^{q} \\ \left(\upsilon\alpha_{s}^{q} + \beta_{s}^{q}\right)\left(r_{s}^{w} + y_{s}^{q} - 1\right) \le c2_{s}^{w,q} \le \left(\upsilon\alpha_{s}^{q} + \beta_{s}^{q}\right)\gamma_{s}^{w} \end{cases} \quad \forall w \in W, s \in S, q \in Q \tag{19}$$

$$c^{w} = \sum_{n=1}^{V(w)} \pi_{n}^{w} c_{n}^{w}, \quad \forall w \in W \tag{20}$$

$$\sum_{n=1}^{V(w)} \pi_{n}^{w} \le z^{w}, \quad \forall w \in W \tag{21}$$

$$\begin{cases} \sum\limits_{n\in H^{+}(\kappa,w)} \pi_{n}^{w} \le \xi_{\kappa}^{w} \\ \sum\limits_{n\in H^{-}(\kappa,w)} \pi_{n}^{w} \le 1 - \xi_{\kappa}^{w} \end{cases} \quad \forall w \in W, \kappa = 1,\ldots,\left\lceil \log_{2}\left(V(w) - 1\right)\right\rceil \tag{22}$$

$$x_{ij}^{w}, y_{s}^{q}, z^{w}, \gamma_{s}^{w} \in \{0,1\}, \quad \forall v \in V, w \in W, s \in S, q \in Q, i, j \in N : (i,j) \in A \tag{23}$$

$$e_{i}^{w}, p_{s}^{w}, \pi_{n}^{w} \in \mathbb{R}_{+}, \quad \forall i \in N, s \in S, w \in W, n = 1,\ldots,V(w) \tag{24}$$

$$\xi_{\kappa}^{w} \in \{0,1\}, \quad \forall w \in W, \kappa = 1,\ldots,\left\lceil \log_{2}\left(V(w) - 1\right)\right\rceil \tag{25}$$

where the sets $H^{+}(\kappa,w)$ and $H^{-}(\kappa,w)$ are defined as follows:

$$H^{+}(\kappa,w) = \left\{ n = 1,\ldots,V(w) \mid \left(n = 1 \wedge \mathbb{G}_{2,\kappa}^{w}\right) \cup \left(\mathbb{G}_{n-1,\kappa}^{w} = 1 \wedge \mathbb{G}_{n,\kappa}^{w} = 1\right) \cup \left(\mathbb{G}_{V(w)-1,\kappa}^{w} = 1 \wedge n = V(w)\right) \right\} \tag{26}$$

$$H^{-}(\kappa,w) = \left\{ n = 1,\ldots,V(w) \mid \left(n = 0 \wedge \mathbb{G}_{2,\kappa}^{w}\right) \cup \left(\mathbb{G}_{n-1,\kappa}^{w} = 0 \wedge \mathbb{G}_{n,\kappa}^{w} = 0\right) \cup \left(\mathbb{G}_{V(w)-1,\kappa}^{w} = 0 \wedge n = V(w)\right) \right\} \tag{27}$$

In the model [OP-II], the feasible travel cost range of OD pair w is partitioned by a total number of $V(w)$ pre-specified breakpoints; the $n-th$ breakpoint of OD pair w is denoted by c_n^w. The flow volume of OD pair w under the travel cost c_n^w is represented by $f^w(c_n^w)$. For each breakpoint $c_n^w, \forall w \in W, n = 1,...,V(w)$, a nonnegative variable π_n^w is defined, referred to as the convex coefficient associated with c_n^w. Eq. (15) represents the approximated covered flow volume. Constraints (16) and (17) limit the total construction costs and the number of station types at a particular location, respectively. Constraint (18) defines the GTC of OD pair w, where $c1_s^{w,q}$ and $c2_s^{w,q}$ are auxiliary variables for linearizing the charging amount-dependent cost and the fixed cost of charging at location s by type q station w. Constraint (19) is the linearization constraint for the variables $c1_s^{w,q}$ and $c2_s^{w,q}$. The GTC of OD pair w is represented by breakpoints and coefficients in Constraint (20). The upper bound of all coefficient of OD pair w is specified by Constraint (21). The coefficients should further satisfy Constraint (22). In the model [OP-II], a Gray code method is employed to reduce the number of auxiliary binary variables in the formulation of the piece-wise linear approximation. A special kind of binary code, namely Gray code, is used to develop a compact form of the coefficient constraint, i.e., Constraint (22). The $\kappa-th$ digit of the $n-th$ Gray code of OD pair w is denoted by $\mathbb{G}_{n,\kappa}^w$. A binary auxiliary variable ξ_κ^w is defined for the $\kappa-th$ digit of the Gray codes of OD pair w. As for the details of the Gray code method, please refer to the paper of Ouyang et al. (2020).

Appendix 4 Pseudo-code of the TSA heuristic algorithm

Initialize T, ε, k, l, L, D^*, f^*, $\bar{D} \leftarrow D^*$, $\bar{f} \leftarrow f^*$, $\bar{v}_s \leftarrow v_s^*, \forall s \in S$, and $X_{Tabu} \leftarrow \varnothing$.
// Outer Layer
For $l = 1,...,L$
  // New deployment generation
    $Out\_of\_Tabu \leftarrow 0$ // Denote whether the new deployment is out of the Tabu list.
    While $Out\_of\_Tabu = 0$
      $\tilde{s} \leftarrow Random\_Min(\bar{D}, k)$ // Find the station to be removed.
      $D' \leftarrow Random\_Strategy(\bar{D}, \tilde{s})$ // Select a new deployment generation strategy.
      If $D' \notin X_{Tabu}$
        $Out\_of\_Tabu \leftarrow 1$ // The new deployment is out of the Tabu list.
      End if
    End while
  // Inner Layer
    // New deployment assessment
    $f' \leftarrow Find\_flow\_coverage(D')$ // Assess the flow coverage of D'.
    $v_s' \leftarrow Find\_passing\_flows(s), \forall s \in S$ // Calculate the flows through each location.
  // Deployment update and annealing
    If $f' > \bar{f}$
      $\bar{D} \leftarrow D'$, $\bar{f} \leftarrow f'$, $\bar{v}_s \leftarrow v_s', \forall s \in S$ // Update the current deployment, flow coverage, and flows through each candidate location.
      If $\bar{f} > f^*$

$D^* \leftarrow \bar{D}$, $f^* \leftarrow \bar{f}$ // Update the best deployment and the best flow coverage.
End if
Else if $e^{(f'-\bar{f})/T} \geq Rand(0,1)$ // Generate a random number between 0 and 1 as the threshold.
$\bar{D} \leftarrow D'$, $\bar{f} \leftarrow f'$, $\bar{v}_s \leftarrow v'_s, \forall s \in S$
$T \leftarrow \varepsilon \cdot T$ // Update the annealing temperature.
Else
$X_{Tabu} \leftarrow X_{Tabu} \bigcup D'$ // Update the Tabu list.
End if
End for
Return D^* // Return the best deployment.

We define several subfunctions for ease of representation. Subfunction $Random\_Min(\bullet)$ returns a candidate location, denoted by $\tilde{s}$, that is randomly chosen from the worst-k locations according to the value of $\bar{v}_s, \forall s \in S$. Subfunction $Random\_Strategy(\bullet)$ returns a new station deployment plan, denoted by D', that is constructed by removing the station at location $\tilde{s}$ from the incumbent deployment plan $\bar{D}$ and randomly chooses a strategy between *Strategy Fast* and *Strategy Slow* to allocate new stations. The flow coverage of deployment plan D' and the flows through each location $v'_s, \forall s \in S$ are obtained by $Find\_flow\_coverage(\bullet)$ and $Find\_passing\_flows(\bullet)$, respectively through the model [OP-I] and the elastic demand function.

References

Araya, D., 2018. China's Belt and Road Initiative is poised to transform the clean energy industry, *The Brookings Institution*. The Brookings Institution, Washington, DC, USA.

Abbasi, M.H., Taki, M., Rajabi, A., Li, L., Zhang, J., 2019. Coordinated operation of electric vehicle charging and wind power generation as a virtual power plant: A multi-stage risk constrained approach. *Applied Energy* 239, 1294-1307.

Caulfield, B., Farrell, S., McMahon, B., 2010. Examining individuals preferences for hybrid electric and alternatively fuelled vehicles. *Transport Policy* 17(6), 381-387.

Chiang, W.-C., Russell, R.A., 1996. Simulated annealing metaheuristics for the vehicle routing problem with time windows. *Annals of Operations Research* 63(1), 3-27.

Chu, W., Im, M., Song, M.R., Park, J., 2019. Psychological and behavioral factors affecting electric vehicle adoption and satisfaction: A comparative study of early adopters in China and Korea. *Transportation Research Part D: Transport and Environment* 76, 1-18.

Commins, N., Nolan, A., 2011. The determinants of mode of transport to work in the Greater Dublin Area. *Transport Policy* 18(1), 259-268.

Eliasson, J., 2021. Efficient transport pricing–why, what, and when? *Communications in Transportation Research*, *1*, 100006.

Felipe, A., Ortuno, M.T., Righini, G., Tirado, G., 2014. A heuristic approach for the green vehicle routing problem with multiple technologies and partial recharges. *Transportation Research Part E: Logistics and Transportation Review* 71, 111-128.

Franke, T., Krems, J.F., 2013. What drives range preferences in electric vehicle users? *Transport Policy* 30, 56-62.

Gao, K., Yang, Y., Qu, X., 2021. Diverging effects of subjective prospect values of uncertian time and money. *Communications in Transportation Research*, *1*, 100007.

Globisch, J., Plötz, P., Dütschke, E., Wietschel, M., 2019. Consumer preferences for public charging infrastructure for electric vehicles. *Transport Policy* 81, 54-63.

Guo, F., Yang, J., Lu, J.Y., 2018. The battery charging station location problem: Impact of users' range anxiety and distance convenience. *Transportation Research Part E: Logistics and Transportation Review* 114, 1-18.

He, J., Yang, H., Tang, T.-Q., Huang, H.-J., 2018. An optimal charging station location model with the consideration of electric vehicle's driving range. *Transportation Research Part C: Emerging Technologies* 86, 641-654.

He, J., Yang, H., Tang, T.-Q., Huang, H.-J., 2020. Optimal deployment of wireless charging lanes considering their adverse effect on road capacity. *Transportation Research Part C: Emerging Technologies* 111, 171-184.

Hodgson, M.J., 1990. A flow capturing location allocation model, *Geographical Analysis*, pp. 270-279.

Hosseini, M., MirHassani, S., 2015. Refueling-station location problem under uncertainty. *Transportation Research Part E: Logistics and Transportation Review* 84, 101-116.

Hosseini, M., MirHassani, S.A., Hooshmand, F., 2017. Deviation-flow refueling location problem with capacitated facilities: Model and algorithm. *Transportation Research Part D: Transport and Environment* 54, 269-281.

IEA, 2017. Global EV Outlook 2017: Two million and counting. The International Energy Agency, Paris, France.

Kim, J.G., Kuby, M., 2012. The deviation-flow refueling location model for optimizing a network of refueling stations. *International Journal of Hydrogen Energy* 37(6), 5406-5420.

Kirkpatrick, S., Gelatt, C.D., Vecchi, M.P., 1983. Optimization by simulated annealing. *Science* 220(4598), 671-680.

Kuby, M., Lim, S., 2005. The flow-refueling location problem for alternative-fuel vehicles. *Socio-Economic Planning Sciences* 39(2), 125-145.

Lebeau, K., Van Mierlo, J., Lebeau, P., Mairesse, O., Macharis, C., 2013. Consumer attitudes towards battery electric vehicles: a large-scale survey. *International Journal of Electric and Hybrid Vehicles* 5(1), 28-41.

Liao, F., Molin, E., Timmermans, H., van Wee, B., 2019. Consumer preferences for business models in electric vehicle adoption. *Transport Policy* 73, 12-24.

Liao, P., Tang, T.-Q., Liu, R., Huang, H.-J., 2021. An eco-driving strategy for electric vehicle based on the powertrain. *Applied Energy* 302, 117583.
Liu, H., Wang, D.Z., 2017. Locating multiple types of charging facilities for battery electric vehicles. *Transportation Research Part B: Methodological* 103, 30-55.
Lu, X.-S., Liu, T.-L., Huang, H.-J., 2015. Pricing and mode choice based on nested logit model with trip-chain costs. *Transport Policy* 44, 76-88.
Masoumi, H.E., 2019. A discrete choice analysis of transport mode choice causality and perceived barriers of sustainable mobility in the MENA region. *Transport Policy* 79, 37-53.
Morrow, K., Karner, D., Francfort, J., 2008. Plug-in Hybrid Electric Vehicle Charging Infrastructure Review, *US Department of Energy-Vehicle Technologies Program*.
Nissa, 2019. Nissa Leaf 2019: Range and Charging.
NREL, 2012. Plug-In electric vehicle handbook for public charging station hosts, *Clean Cities Technical Response Service*, pp. 1-20.
Osman, I.H., 1993. Metastrategy simulated annealing and tabu search algorithms for the vehicle routing problem. *Annals of Operations Research* 41(4), 421-451.
Ouyang, X., Xu, M., Zhou, B., 2021. A multi-type charging station location model for electric vehicle users considering partial charging behavior and nonlinear elastic demand. *Networks and Spatial Economics* (accepted).
Owen, S.H., Daskin, M.S., 1998. Strategic facility location: A review. *European Journal of Operational Research* 111(3), 423-447.
Revelle, C., 1993. Facility Siting and Integer-Friendly Programming. *European Journal of Operational Research* 65, 147-158.
Schiffer, M., Walther, G., 2017. The electric location routing problem with time windows and partial recharging. *European Journal of Operational Research* 260(3), 995-1013.
She, Z.-Y., Qing Sun, Ma, J.-J., Xie, B.-C., 2017. What are the barriers to widespread adoption of battery electric vehicles? A survey of public perception in Tianjin, China. *Transport Policy* 56, 29-40.
Soltani-Sobh, A., Heaslip, K., Stevanovic, A., Bosworth, R., Radivojevic, D., 2017. Analysis of the electric vehicles adoption over the United States. *Transportation Research Procedia* 22, 203-212.
Souche, S., 2010. Measuring the structural determinants of urban travel demand. *Transport Policy* 17(3), 127-134.
Sun, Z., Gao, W., Li, B., Wang, L., 2018. Locating charging stations for electric vehicles. *Transport Policy* (in press).
Upchurch, C., Kuby, M., Lim, S., 2009. A model for location of capacitated alternative-fuel stations, *Geographical Analysis*.
Van Laarhoven, P.J., Aarts, E.H., 1987. *Simulated annealing: Theory and applications*. Springer, pp. 7-15.
Wang, F., Zhang, J., Xu, X., Cai, Y., Zhou, Z., Sun, X., 2019. A comprehensive dynamic efficiency-enhanced energy management strategy for plug-in hybrid electric vehicles. *Applied energy* 247, 657-669.
Wee, S., Coffman, M., Allen, S., 2020. EV driver characteristics: Evidence from Hawaii. *Transport Policy* 87, 33-40.
XinhuaNet, 2020. State Grid Zhejiang electric power accelerates construction and upgrading of charging piles, *XinhuaNet of China*.
Xu, M., Meng, Q., 2020. Optimal deployment of charging stations considering path deviation and nonlinear elastic demand. *Transportation Research Part B: Methodological* 135, 120-142.
Xu, M., Meng, Q., Liu, K., Yamamoto, T., 2017. Joint charging mode and location choice model for battery electric vehicle users. *Transportation Research Part B: Methodological* 103, 68-86.
Xu, M., Meng, Q., Liu, Z.Y., 2018. Electric vehicle fleet size and trip pricing for one-way carsharing services considering vehicle relocation and personnel assignment. *Transportation Research Part B-Methodological* 111, 60-82.
Xu, M., Yang, H., Wang, S.A., 2020. Mitigate the range anxiety: Siting battery charging stations for electric vehicle drivers. *Transportation Research Part C: Emerging Technologies* 114, 164-188.
Yang, H., Huang, H.J., 1997. Analysis of the time-varying pricing of a bottleneck with elastic demand using optimal control theory. *Transportation Research Part B: Methodological* 31(6), 425-440.

Yilmaz, M., Krein, P.T., 2012. Review of battery charger topologies, charging power levels, and infrastructure for plug-in electric and hybrid vehicles. *IEEE Transactions on Power Electronics* 28(5), 2151-2169.

Zhang, J., Tang, T.-Q., Yan, Y., Qu, X., 2021. Eco-driving control for connected and automated electric vehicles at signalized intersections with wireless charging. *Applied Energy* 282, 116215.

Zhang, J., Yan, J., Liu, Y., Zhang, H., Lv, G., 2020a. Daily electric vehicle charging load profiles considering demographics of vehicle users. *Applied Energy* 274, 115063.

Zhang, Y., Liu, X., Wei, W., Peng, T., Hong, G., Meng, C., 2020b. Mobile charging: A novel charging system for electric vehicles in urban areas. *Applied Energy* 278, 115648.

Zheng, H., He, X., Li, Y., Peeta, S., 2017. Traffic equilibrium and charging facility locations for electric vehicles. *Networks and Spatial Economics* 17(2), 435-457.